



**HAL**  
open science

## Proteomic differences in the hippocampus and cortex of epilepsy brain tissue

Geoffrey Pires, Dominique Leitner, Eleanor Drummond, Evgeny Kanshin, Shruti Nayak, Manor Askenazi, Arline Faustin, Daniel Friedman, Ludovic Debure, Beatrix Ueberheide, et al.

► **To cite this version:**

Geoffrey Pires, Dominique Leitner, Eleanor Drummond, Evgeny Kanshin, Shruti Nayak, et al.. Proteomic differences in the hippocampus and cortex of epilepsy brain tissue. *Brain Communications*, 2021, 3 (2), 10.1093/braincomms/fcab021 . hal-03270273

**HAL Id: hal-03270273**

<https://hal.sorbonne-universite.fr/hal-03270273v1>





Submitted on 24 Jun 2021

**HAL** is a multi-disciplinary open access archive for the deposit and dissemination of scientific research documents, whether they are published or not. The documents may come from teaching and research institutions in France or abroad, or from public or private research centers.

L'archive ouverte pluridisciplinaire **HAL**, est destinée au dépôt et à la diffusion de documents scientifiques de niveau recherche, publiés ou non, émanant des établissements d'enseignement et de recherche français ou étrangers, des laboratoires publics ou privés.

# BRAIN COMMUNICATIONS

## Proteomic differences in the hippocampus and cortex of epilepsy brain tissue

 **Geoffrey Pires**,<sup>1,2,3,\*</sup>  **Dominique Leitner**,<sup>1,\*</sup>  **Eleanor Drummond**,<sup>2,4</sup> **Evgeny Kanshin**,<sup>5</sup> **Shruti Nayak**,<sup>5</sup> **Manor Askenazi**,<sup>6,7</sup> **Arline Faustin**,<sup>2</sup> **Daniel Friedman**,<sup>1</sup> **Ludovic Debure**,<sup>2</sup> **Beatrix Ueberheide**,<sup>2,5,7</sup>  **Thomas Wisniewski**<sup>2,8,9</sup> and **Orrin Devinsky**<sup>1</sup>

\* These authors contributed equally to this work.

Epilepsy is a common neurological disorder affecting over 70 million people worldwide, with a high rate of pharmaco-resistance, diverse comorbidities including progressive cognitive and behavioural disorders, and increased mortality from direct (e.g. sudden unexpected death in epilepsy, accidents, drowning) or indirect effects of seizures and therapies. Extensive research with animal models and human studies provides limited insights into the mechanisms underlying seizures and epileptogenesis, and these have not translated into significant reductions in pharmaco-resistance, morbidities or mortality. To help define changes in molecular signalling networks associated with seizures in epilepsy with a broad range of aetiologies, we examined the proteome of brain samples from epilepsy and control cases. Label-free quantitative mass spectrometry was performed on the hippocampal cornu ammonis 1–3 region (CA1–3), frontal cortex and dentate gyrus microdissected from epilepsy and control cases ( $n = 14/\text{group}$ ). Epilepsy cases had significant differences in the expression of 777 proteins in the hippocampal CA1 – 3 region, 296 proteins in the frontal cortex and 49 proteins in the dentate gyrus in comparison to control cases. Network analysis showed that proteins involved in protein synthesis, mitochondrial function, G-protein signalling and synaptic plasticity were particularly altered in epilepsy. While protein differences were most pronounced in the hippocampus, similar changes were observed in other brain regions indicating broad proteomic abnormalities in epilepsy. Among the most significantly altered proteins, G-protein subunit beta 1 (GNB1) was one of the most significantly decreased proteins in epilepsy in all regions studied, highlighting the importance of G-protein subunit signalling and G-protein-coupled receptors in epilepsy. Our results provide insights into common molecular mechanisms underlying epilepsy across various aetiologies, which may allow for novel targeted therapeutic strategies.

- 1 Comprehensive Epilepsy Center, New York University Grossman School of Medicine, New York, NY, USA
- 2 Department of Neurology, Center for Cognitive Neurology, New York University Grossman School of Medicine, New York, NY, USA
- 3 Alzheimer's and Prion Diseases Team, Paris Brain Institute, CNRS, UMR 7225, INSERM 1127, Sorbonne University UM75, Paris, France
- 4 Faculty of Medicine and Health, Brain and Mind Centre and School of Medical Sciences, University of Sydney, Sydney, Australia
- 5 Proteomics Laboratory, Division of Advanced Research Technologies, New York University Grossman School of Medicine, New York, NY, USA
- 6 Biomedical Hosting LLC, USA
- 7 Department of Biochemistry and Molecular Pharmacology, New York University Grossman School of Medicine, New York, NY, USA
- 8 Department of Psychiatry, New York University Grossman School of Medicine, New York, NY, USA
- 9 Department of Pathology, New York University Grossman School of Medicine, New York, NY, USA

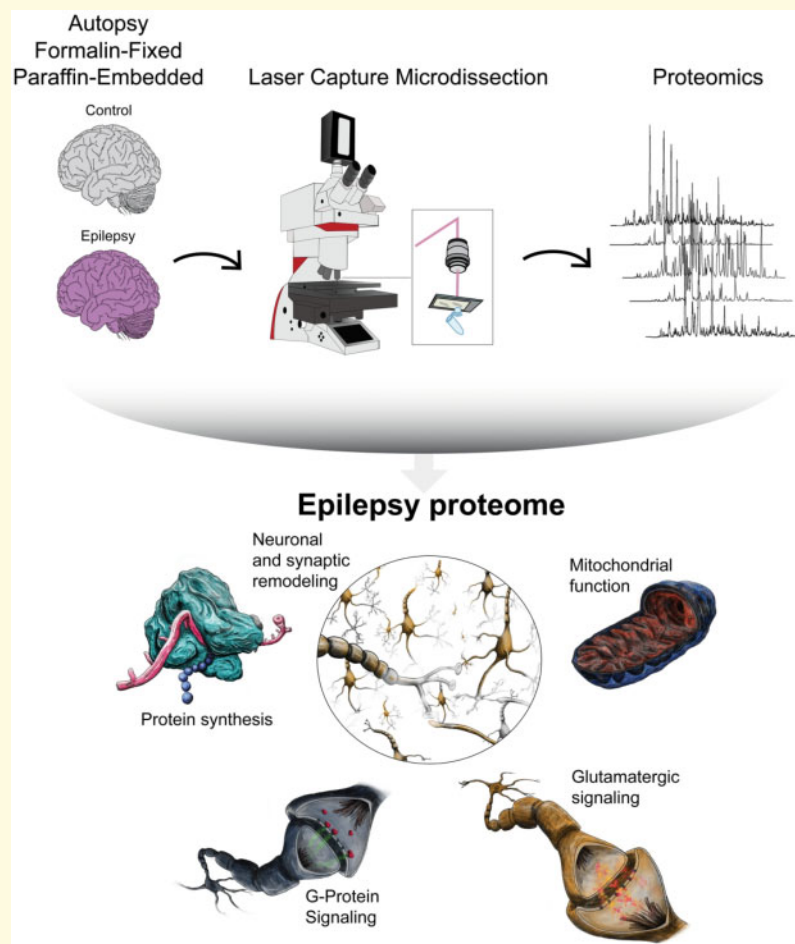
Correspondence to: Thomas Wisniewski  
 Professor of Neurology  
 Pathology and Psychiatry at NYU Grossman School of Medicine  
 Science Building, Rm 1017  
 435 East 30th Street  
 New York, NY 10016, USA  
 E-mail: thomas.wisniewski@nyulangone.org

Correspondence may also be addressed to: Orrin Devinsky  
 Professor of Neurology, Neuroscience and Neurosurgery at NYU Grossman School of Medicine  
 223 East 34th Street  
 New York, NY 10016, USA  
 E-mail: orrin.devinsky@nyulangone.org

**Keywords:** epilepsy; seizures; proteomics; synaptophysin

**Abbreviations:** ASD = anti-seizure drug; CBZ = carbamazepine; CLB = clobazam; CLO = clonazepam; COD = cause of death; CSF = Cerebrospinal fluid; DDG = dysgenesis of the dentate gyrus; DG = dentate gyrus; ESL = eslicarbazepine; FBM = felbamate; FC = frontal cortex; FCD = focal cortical dysplasia; FDR = false discovery rate; FFPE = formalin fixed paraffin embedded; fPHT = fosphenytoin; GBP = gabapentin; HIPP = hippocampus; HP = hippocampus; Hr = hour(s); HS = hippocampal sclerosis; IPA = Ingenuity Pathway Analysis; LAC = lacosamide; LCM = laser capture microdissection; LAM = lamotrigine; LEV = levetiracetam; LOR = lorazepam; MCA/ACA = middle cerebral artery/anterior cerebral artery; MTLE = mesial temporal lobe epilepsy; MTLE + HS = mesial temporal lobe epilepsy with hippocampal sclerosis; MS = mass spectrometry; ND = not determined; PCA = principal component analysis; PER = perampanel; PHT = phenytoin; PMI = post-mortem interval; TPM = topiramate; VPA = valproate; Yr = year(s)

### Graphical Abstract



## Introduction

Epilepsy is a spectrum disorder with diverse aetiologies and outcomes affecting over 70 million people worldwide.<sup>1–4</sup> Aetiologies include ion channel and many other genetic mutations, infection, structural lesions, metabolic abnormalities and autoimmune disorders, although the cause remains unknown in many cases.<sup>5–9</sup> The mechanisms underlying ictogenesis and epileptogenesis alter the balance of excitation and inhibition.<sup>10</sup> Anti-seizure drugs (ASDs) target multiple mechanisms, including ion channels (e.g. sodium, calcium, potassium), neurotransmitter receptors and metabolism (e.g. GABA-A receptors, GABA transporter 1, GABA transaminase), synaptic vesicles (e.g. SV2A) and regulators of cell growth (e.g. mTOR inhibition). However, since one-third of patients have an incomplete response to ASDs, dietary, neuromodulatory and resective or disconnective surgical procedures, a broader understanding of the cellular and molecular drivers of ictogenesis and epileptogenesis is essential to identify new therapeutic targets.<sup>4,11,12</sup>

Human and animal epilepsy studies reveal that seizures can arise from neocortical or limbic lesions, including focal cortical dysplasia (FCD), hippocampal sclerosis, tumours, inflammation and vascular lesions.<sup>13–15</sup> The hippocampus is often involved in focal epilepsy as a primary (e.g. mesial temporal lobe epilepsy [MTLE]) or secondary seizure focus (e.g. areas robustly connected with entorhinal cortex and hippocampus). The hippocampal cornu ammonis (CA) CA1–4 region and dentate gyrus are involved in seizure generation and in hippocampal sclerosis.<sup>16</sup>

To date, our knowledge of brain protein changes in epilepsy comes from experimental MTLE models and human brain tissue. The most robust changes in epilepsy brain tissue involve proteins related to neurotransmitters, cell signalling, glucose metabolism and protein synthesis.<sup>17,18</sup> Genomic, epigenetic and transcriptomic studies have revealed insights into mechanisms underlying ictogenesis and epileptogenesis by identifying novel genetic loci and profound changes in gene expression in humans and animal models.<sup>19–24</sup> However, the poor correlation between RNA expression and protein levels limits the value of isolated transcriptomic or genomic studies.<sup>25</sup> Unbiased, mass spectrometry-based proteomic studies of human epilepsy tissue can complement these studies, particularly since proteins are direct drug targets. Proteomics provides a global view of protein changes at a functional or network level. The majority of previous epilepsy proteomics studies have examined animal model tissue, rather than human brain tissue.<sup>26,27</sup> Two previous studies have performed proteomics on human epilepsy brain tissue, however, these were limited by either small numbers, analysis of single regions or low sensitivity proteomics approaches. These studies identified 77 proteins differentially expressed in MTLE hippocampi compared with controls<sup>28</sup> and 18 differentially expressed proteins between high- and low-spiking regions in six epilepsy

patients.<sup>29</sup> We hypothesized that we would identify more extensive protein differences in epilepsy by using a more sensitive proteomic approach, and that we would generate novel insight into the pathophysiology of epilepsy by examining protein changes in multiple brain regions that are differentially affected in epilepsy.

Recent advances in proteomics methods have shown that proteomics can be successfully performed using formalin fixed paraffin embedded (FFPE) tissue.<sup>30,31</sup> We recently developed a new method combining laser capture microdissection (LCM) and mass spectrometry that allows localized proteomics using microdissected FFPE tissue to more precisely evaluate protein differences in microscopic brain regions or pathological lesions rather than bulk tissue.<sup>30,31</sup> We specifically optimized this technique to allow the use of FFPE tissue so that archived human tissue specimens collected at autopsy could be used. This is a particular advantage of our approach, as the vast majority of autopsy human tissue specimens are FFPE blocks, which are currently an underutilized, but exceptionally valuable resource for research.

Therefore, to advance our knowledge of proteomics that is common to human epilepsy syndromes, we applied this method to epilepsy and control human brains across three regions: CA1–3 of the hippocampus, the dentate gyrus, and the frontal cortex.

## Materials and methods

### Ethics statement

All studies were approved by the Institutional Review Board (IRB) at New York University (NYU). In all cases, written informed consent was obtained from the legal guardian or patient, and material used had ethical approval. All patient data and samples were deidentified and stored according to NIH guidelines.

### Human brain tissue

All human tissue samples were collected at autopsy. Epilepsy and control cohorts were studied. The epilepsy cases ( $n=14$ ) were acquired through the North American SUDEP Registry (NASR) and included cases from multiple sites around the country whose cause of death (COD) was not SUDEP. The control cases ( $n=14$ ) were acquired through the NYU autopsy service. All control and epilepsy neuropathology reports were performed and finalized at the NYU Pathology Department. Histological evaluation of all cases was performed by neuropathologists and findings were classified using the international consensus criteria.<sup>2,13,32</sup> Storage, as well as sample processing (sample collection, embedding, archival and sectioning) was performed for all control and epilepsy cases per the NYU Pathology Department protocol. For proteomics analyses, specimens were retrieved from the Center for Biospecimen Research and Development (CBRD). The NYU Experimental

**Table 1 Control case information**

Case	Age	Sex	COD	PMI (hr)	Significant neuropathology	Brain region
1	55	M	Cardiac arrest	64		HP, DG, FC
2	57	M	Cardiac arrest	142		HP, DG, FC
3	56	F	Cardiac arrest	46		HP, DG, FC
4	49	F	Cardiac arrest	144		HP, DG, FC
5	59	F	Cardiac arrest	57		HP, DG, FC
6	59	M	Possible cardiac arrest	116		HP, DG, FC
7	57	M	Cardiac arrest	91		HP, DG, FC
8	55	M	Pulmonary fibrosis	57	Subacute, right temporal white matter microinfarct	HP, DG, FC
9	59	M	Cardiac arrest	60		HP, DG, FC
10	38	M	Anoxic encephalopathy secondary to cardiac arrest	44	Acute and chronic hypoxic-ischaemic changes, diffuse	HP, DG, FC
11	59	M	Supraglottic squamous cell carcinoma	<120	Ischaemic infarct, left frontal MCA/ACA	HP, DG, FC
12	49	M	Cardiac arrest	48	Meningeal fibrosis	HP, DG, FC
13	50	M	Possible cardiac arrest (contributing—acute gastroenteritis)	50	Hypoxic-ischaemic changes, diffuse	HP, DG, FC
14	54	M	Cardiac arrest	66	Hypoxic-ischaemic injury, acute, multifocal	HP, DG, FC

COD = cause of death; PMI = post-mortem interval; h = hour; HP = hippocampus; DG = dentate gyrus; FC = frontal cortex; ACA = anterior cerebral artery; MCA = middle cerebral artery.

**Table 2 Epilepsy case information**

Case	Age	Sex	COD	PMI (hr)	Significant neuropathology	Disease duration (yr)	Seizure type	ASDs at time of death	Brain region
1	50	M	Choking on foreign object	15		49.5	Focal	none	FC
2	34	F	Pulmonary embolism	13	FCD-IIA	32	Focal	none	HP, DG, FC
3	45	M	Suicide	27	DDG	20	Focal	FBM, LAM, LOR, VPA	HP, DG
4	36	M	Drowning	48	HS	12	Focal	PHT, LAM, CBZ, ESL	HP, DG, FC
5	36	M	Overdose/intoxication	20		8	ND	PHT, LEV	HP, DG, FC
6	54	M	Accident/trauma	<24	Mild gliosis, contusion, focal cortical disorganization	1	ND	PHT	HP, DG
7	64	F	Overdose	18		ND	ND	PHT	HP, DG
8	9	F	Drowning	30	FCD-IIA	8	ND	LAM, PHT	HP, DG
9	45	M	Suicide	<48		43	ND	CLB, GBP	HP, DG, FC
10	24	F	Drowning	<48	DDG	ND	ND	LEV, VPA, PER, CBZ, CLO, LOR	HP, DG, FC
11	28	M	Accident/trauma	<48	DDG	22	ND	CBZ, LAC	HP, DG, FC
12	23	M	Drowning	<48	FCD-IA	ND	ND	VPA, TPM, CLO	HP, DG, FC
13	32	M	Ethanol intoxication and clobazam overdose	19	FCD-IIA, Wernicke's encephalopathy	10	ND	LAM, LOR, PHT	HP, DG, FC
14	49	M	Aspiration	43	DDG, HS, gliosis, hemisphere atrophy	48.4	ND	fPHT	HP, DG, FC

COD = cause of death; PMI = post-mortem interval; h = hour; yr = year; HP = hippocampus; DG = dentate gyrus; FC = frontal cortex; FCD = focal cortical dysplasia; HS = hippocampal sclerosis; DDG = dysgenesis of the dentate gyrus; ND = not determined; ASD = anti-seizure drug; CBZ = carbamazepine; CLB = clobazam; CLO = clonazepam; ESL = eslicarbazepine; FBM = felbamate; fPHT = fosphenytoin; GBP = gabapentin; LAC = lacosamide; LAM = lamotrigine; LEV = levetiracetam; LOR = lorazepam; PER = perampamil; PHT = phenytoin; TPM = topiramate; VPA = valproate.

Pathology Research Laboratory sectioned all cases for LCM and CBRD sectioned all cases for immunohistological validation. Six cases did not have seizure frequency and ten cases seizure type information, which came from a population with health care disparities that were not under regular medical care and therefore had limited medical records. Regarding epilepsy syndrome, there was a broad

representation of various epilepsies in the cases with known clinical information, the majority of which excluded known frontal lobe involvement. All cases were matched for sex and age ( $46 \pm 14$  years) to the best of our ability. Individual patient information [sex, age, COD, post-mortem interval (PMI) and seizure classification if applicable] is included in Tables 1 and 2.

## Laser capture microdissection

We sampled brain tissue from FFPE blocks of hippocampus or superior frontal gyrus collected and processed for autopsy neuropathology. LCM was performed using our published protocol.<sup>30,31,33</sup> Briefly, 8  $\mu\text{m}$ -thick FFPE sections containing hippocampus or superior frontal gyrus were collected onto LCM PET Frame Slides (Leica). Sections were stained with Cresyl violet to visualize neurons and regions of interest (ROIs). For each sample, 10  $\text{mm}^2$  of hippocampus (including CA1–3) and superior frontal gyrus (including layers I–IV) and 4  $\text{mm}^2$  of dentate gyrus (granule cell layer) were microdissected in separate tubes using a LMD6500 microscope at 5 $\times$  magnification (Leica) (Fig. 1). ROIs were collected into ultrapure Pierce Water, LC–MS Grade (ThermoScientific). After collection, samples were centrifuged at 14 000g for 2 min and stored at  $-80^\circ\text{C}$  until peptide extraction.

## Label-free quantitative mass spectrometry proteomics

The study included six experimental groups based on two states (epilepsy, control) and three brain regions. Samples were processed and analysed using label-free quantitative mass spectra (MS) in three batches: hippocampus ( $n=13$  epilepsy,  $n=14$  controls), frontal cortex ( $n=11$  epilepsy,  $n=14$  control) and dentate gyrus ( $n=13$  epilepsy,  $n=14$  control). The same epilepsy and control cases were used in the three batches. For each ROI analysed, samples were prepared for label-free quantitative MS.<sup>30,31</sup> Samples were thawed at room temperature (RT) and resuspended by adding 50  $\mu\text{l}$  of 100 mM ammonium bicarbonate and 20% acetonitrile solution to the cap and the tube spun down. This step was repeated three more times to ensure thorough cap washing. Samples were then incubated at  $95^\circ\text{C}$  for 1 h followed by a  $65^\circ\text{C}$  incubation for 2 h. Reduction was performed using dithiothreitol at  $57^\circ\text{C}$  for 1 h (2  $\mu\text{l}$  of 0.2 M) followed by alkylation with iodoacetamide at RT in the dark for 45 min (2  $\mu\text{l}$  of 0.5 M). The samples were subsequently digested with 300 ng of sequencing grade modified trypsin (Promega) overnight at RT with gentle shaking. After digestion samples were acidified with trifluoroacetic acid to a pH of 2 and peptides were desalted using POROS R2 C18 beads as previously described.<sup>30,31,33</sup> The samples were resuspended in 0.5% acetic acid and stored at  $-80^\circ\text{C}$  until further analysis. Aliquots of the sample were loaded onto an Acclaim PepMap 100 (75  $\mu\text{m} \times 2\text{ cm}$ ) precolumn connected to a PepMap RSLC C18 (2  $\mu\text{m}$ , 100 A  $\times$  50 cm) analytical column using the autosampler of an EASY-nLC 1200 (ThermoScientific). The samples were gradient eluted directly into an Orbitrap Fusion Lumos mass spectrometer (ThermoScientific) using a 165 min gradient (Solvent A consisting of 2% acetonitrile in 0.5% acetic acid and Solvent B of 80% acetonitrile in 0.5% acetic

acid). High resolution full MS were acquired with a resolution of 240,000, an automatic gain control (AGC) target of  $1\text{e}6$ , a maximum ion time of 50 ms, and a scan range of 400–1500  $\text{m/z}$ . After each full MS, MS/MS HCD spectra were acquired in the ion trap. All MS/MS spectra were collected using the following: ion trap scan rate Rapid, AGC target of  $2\text{e}4$ , maximum ion time of 18 ms, one microscan, 2  $\text{m/z}$  isolation window, fixed first mass of 110  $\text{m/z}$  and NCE of 32.

## Proteomics computational analysis

MS data were analysed using MaxQuant<sup>34,35</sup> software version 1.6.3.4 and searched against the SwissProt subset of the *H. sapiens* Uniprot database (<http://www.uniprot.org/>) containing 20,365 entries (February 2019 release) to which 248 common laboratory contaminants were added. The enzyme specificity was set to trypsin with a maximum number of missed cleavages set to 2. Peptide identification was performed with an initial precursor mass deviation of 7 ppm and a fragment mass deviation of 20 ppm with subsequent non-linear mass recalibration.<sup>36</sup> Oxidation of methionine residues was searched as variable modification; carbamidomethylation of cysteines was searched as a fixed modification. The false discovery rate (FDR) for peptide, protein and site identification was set to 1% and was calculated using a decoy database approach. The minimum peptide length was set to 6. The option match between runs (1 min time tolerance) was enabled to correlate identification and quantitation results across different runs. Protein quantification was performed with built-in MaxQuant LFQ algorithm<sup>37</sup> with the following settings: minimum ratio count of 2, 'fastLFQ' option enabled, minimum/average number of neighbours 3/6. LFQ normalization was performed within sample groups that belong to the same brain region.

For subsequent statistical analyses we limited our data set to proteins quantified in at least eight samples in at least one of the conditions/brain region (57–72% of microdissected samples, depending on the region analysed). All common contaminant entries were removed, resulting in a matrix with 3216 protein groups. Data analysis used Perseus v. 1.6.2.3.<sup>38</sup> (<http://www.perseus-framework.org/>) using R environment for statistical computing and graphics (<http://www.r-project.org/>). Protein interaction networks and enrichment analyses were done in STRING<sup>39,40</sup> v. 11.0 (<https://string-db.org/>).

## Statistical analyses and interpretation of results

For principal component analysis (PCA) missing values were imputed from a normal distribution with width 0.3 and downshift 1.8 using Perseus. Hierarchical clustering was used to visualize sample metadata in the context of a clustering of those proteins associated with disease (whether positively or negatively, with a 5% FDR),

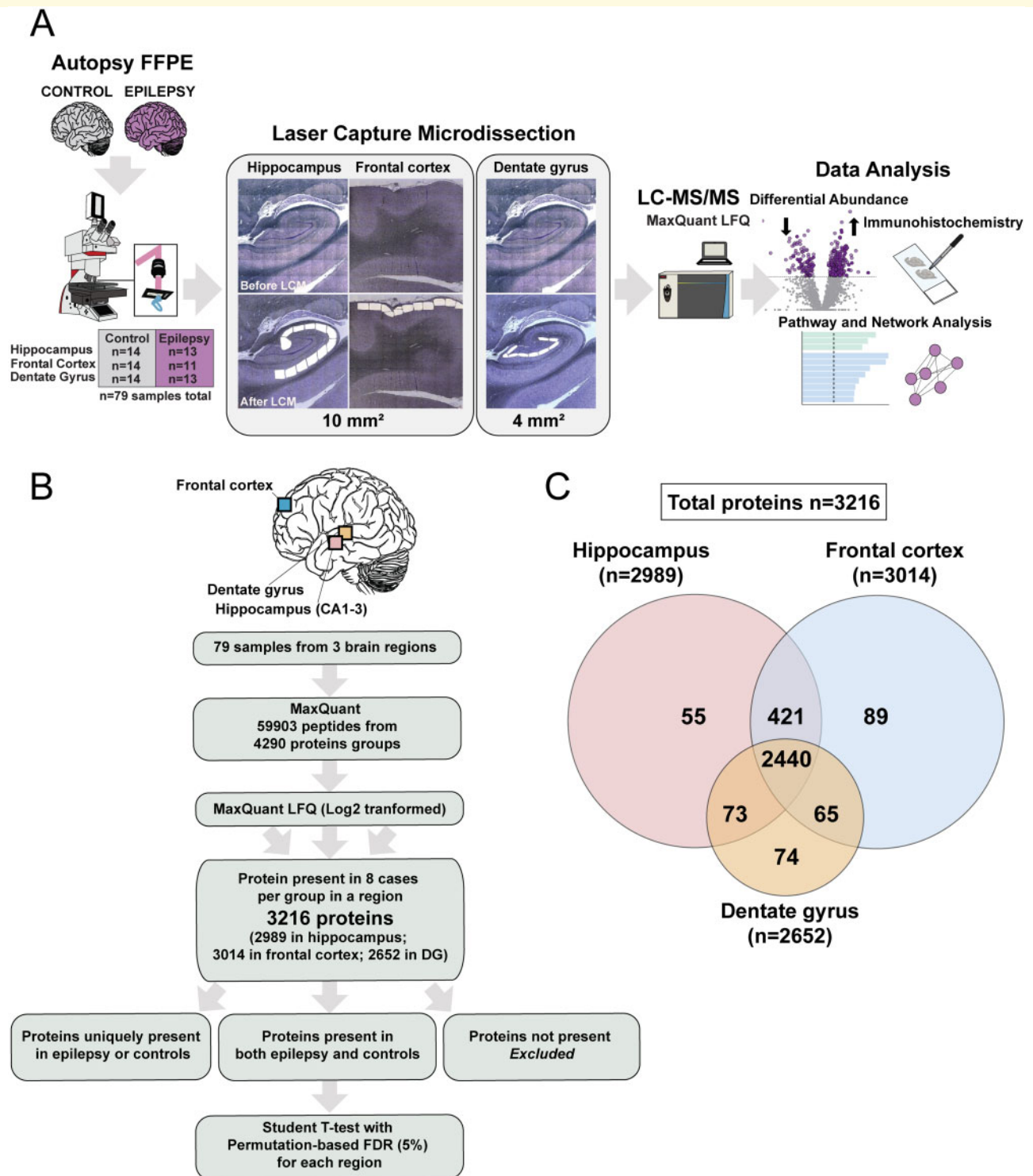


**Figure 1** Quantitative proteomics analysis of epilepsy and non-epilepsy control cases. **(A)** Experimental workflow. Specific protein regions were excised by laser capture microdissection (LCM) from FFPE autopsy brain tissue from control and epilepsy cases ( $n = 14$  in each group) and proteins quantified by label-free quantitative mass spectrometry (MS). Statistical, pathway and network analyses were performed to identify proteins differing in these regions. Three regions were analysed [hippocampus CA1–3 ( $n = 14$  control,  $n = 13$  epilepsy), frontal cortex ( $n = 14$  control,  $n = 11$  epilepsy) and dentate gyrus ( $n = 14$  control,  $n = 13$  epilepsy)]. Validation of protein differences was performed using immunohistochemistry (IHC). **(B)** LC–MS/MS computational analysis. Proteins groups were filtered and quantified using MaxQuant. **(C)** Venn diagram of proteins identified in each region. A total of 3216 protein groups were detected across all brain regions by MS, with 2440 overlapping protein groups between the three regions and 2861 overlapping protein groups between the hippocampus and the frontal cortex.

following a preliminary kmeans clustering using  $k=2$  and the Hartigan and Wong algorithm using the *ComplexHeatmap* package in the R environment.<sup>41</sup> For the hierarchical clustering, Euclidean distance was used as the distance measure and complete-linkage was used to combine clusters. Two-sample Student's *t*-test was used to find differentially expressed proteins between epilepsy and control groups (per each ROI). We corrected for multiple hypothesis testing by calculating the permutation-based FDR ( $n=250$ ). Only protein groups with FDR <5% were deemed significantly different between groups (Supplementary Tables 5–11). For each ROI, protein groups absent in one of the disease groups but present in at least eight cases in the other disease group were by definition considered as differentially expressed (i.e. protein group absent in all control cases but present in at least eight epilepsy cases in the hippocampus was considered as increased in epilepsy in the hippocampus). These significant protein groups are included in Supplementary Table 12.

## Pathway and network analysis

The genes encoding protein groups significantly altered in epilepsy and control were analysed using Ingenuity Pathway Analysis (IPA, Qiagen). We analysed all differentially expressed proteins in the hippocampus ( $n=777$ ), frontal cortex (249) or dentate gyrus ( $n=49$ ). We also analysed differentially expressed proteins in both hippocampus and frontal cortex ( $n=134$ ) and differentially expressed proteins specific to hippocampus or frontal cortex. All pathway analyses are included in Supplementary Tables 16–21. Network analysis was performed using STRING (v.11). Visualization and analysis of the network was conducted via Cytoscape.

## Cell-type specificity

For each ROI, genes encoding all significantly altered proteins in epilepsy and controls were assigned cell-type specificity derived from Lake et al.,<sup>42</sup> in which each gene had only one cell type annotation from any brain region excluding the cerebellum with 1066 possible annotations. For each ROI, cell type enrichment analysis included the following annotations: neurons, excitatory and inhibitory neurons, astrocytes, endothelial, microglia, and oligodendrocytes. The 'neurons' annotation was given to proteins for which the gene in Lake et al. had both 'excitatory neuron' and 'inhibitory neuron' annotations, with no other cell type associated annotations. For the hippocampus, synaptic proteins were assigned based on the classification of 'Synaptic protein' in Lleo et al.<sup>43</sup> Proteins with a neuron cell type annotation and assigned a synaptic protein were referred to as 'neuro-synaptic'.

## Immunohistochemistry

To validate proteomics data, we immunostained FFPE tissue sections as described.<sup>31</sup> Sections were incubated overnight at 4°C with either anti-SYP (synaptic protein synaptophysin) antibody (1:50, abcam, catalogue #ab8049) or anti-TUJ1 antibody (1:300, Biolegend, catalogue #802001). Sections were then incubated for 2 h at RT with fluorescent secondary antibodies (all diluted 1:500, Jackson ImmunoResearch) and coverslipped (ProLongDiamond Antifade Mountant, Invitrogen). All immunostained sections from one immunostaining combination were scanned at 20× magnification on a NanoZoomer HT2 (Hamamatsu) microscope using the same settings. Fiji was used to analyse images with the same threshold for area positive for pixels relative to total area and reported as a percentage. Statistical analyses used unpaired *t*-tests. Representative images were obtained by confocal imaging using a Zeiss 700 confocal microscope. For each immunostaining combination, z-stacked images were collected with the same settings at 20× and 63× magnification with a 13 and 11 μm z-step and are depicted as a maximum projection image.

## Data availability

The mass spectrometry raw files are accessible under MassIVE ID: MSV000085517.

## Results

### Quantitative proteomic analysis of epilepsy and non-epilepsy control cases

To identify proteomic alterations as a result of various aetiologies and seizures in the epilepsy brain, regions of the hippocampus (CA1–3 region) and frontal cortex were microdissected from all epilepsy and control cases (Fig. 1A). Cases were matched for sex, age ( $46 \pm 14$  years) and formalin archival time ( $2 \pm 1$  years) to the best of our ability (Tables 1 and 2). Histological evaluation of all epilepsy cases identified FCD in 4/14 cases, dysgenesis of the dentate gyrus (DDG) in 4/14 cases and hippocampal sclerosis (HS) in 2/14 cases (Tables 1 and 2). Control cases had no significant neuropathology (Tables 1 and 2). Regarding antiepileptic drug treatment, 12 epilepsy cases were prescribed at least 1 ASD (Tables 1 and 2). Regarding ASD adherence, 2/12 cases were known to be taking medications as prescribed, while 3/12 were unknown, and 7/12 were non-adherent for at least one ASD.

Given the role of the dentate gyrus in epileptogenesis and epileptic neuropathology,<sup>44,45</sup> we microdissected and analysed the dentate gyrus proteome separately from CA1–3. Given the reduced size of the dentate gyrus, these samples were smaller than hippocampus and frontal cortex samples (4 mm<sup>2</sup> versus 10 mm<sup>2</sup>; Fig. 1A) and may explain the



lower number of protein groups identified and higher coefficient of variation in dentate samples.

Combined, we analysed 79 samples from 28 cases using label-free quantitative MS and identified 59 903 peptides mapping to 4,894 protein groups (Fig. 1B). Additional filtering based on a minimum of 8 cases with quantification per group in an ROI resulted in 3,216 proteins groups being included in our analyses: frontal cortex—3014, hippocampus—2989 and dentate gyrus—2652 protein groups. The proteins identified overlapped extensively across regions (Fig. 1C).

## Proteomic differences in epilepsy and control cases in hippocampus (CAI–3) and frontal cortex

Protein expression differences between epilepsy and controls were identified in the hippocampus and frontal cortex. PCA showed a striking separation of epilepsy and control groups in hippocampus (permutation-based test,  $P = 2.1 \times 10^{-5}$ , Fig. 2A), and to a lesser extent, in frontal cortex ( $P = 0.002$ ; Fig. 2A) in PC1, confirming that the hippocampus is a more impacted region than the frontal cortex. Presence of FCD, DDG and HS did not account for this separation (Fig. 2A). Supervised hierarchical clustering revealed robust clustering for all hippocampi and frontal cortices from epilepsy cases, consistent with the PCA (Fig. 2B). Variables such as age, sex and neuropathological findings did not drive the clustering (Fig. 2B). Only age of epilepsy onset separated different epilepsy cases in the heatmap: cases with an age of onset below or above 20 years old clustered separately. However, several cases did not have comprehensive clinical information. Those cases came from a population with health care disparities that were not under regular medical care and therefore had limited medical records.

Differentially expressed proteins between epilepsy and controls were determined using Student's *t*-test and Permutation based 5% FDR. There were significant alterations in the expression of 777 proteins in the hippocampus and 296 proteins in the frontal cortex (Fig. 3A and B; Supplementary Tables 7 and 9). A total of 134 proteins were significantly altered in both regions (Supplementary Table 13). The top 20 most significantly altered proteins in epilepsy by region are presented in Tables 3 and 4. Of the 40 top altered proteins, 30 (75%) have been associated with epilepsy in humans or animal models (Tables 3 and 4; Supplementary Tables 1 and 2). We observed that several altered proteins were encoded by genes in which mutations cause epilepsy,<sup>7</sup> including proteins SCN2A, SCN8A, STXBP1, GABBR1, GABBR2, GABRA1, SLC25A12, SLC25A22, SLC6A1 and SCARB2 (Fig. 3C).

We sought to determine whether protein differences in epilepsy were cell type specific. Of the 777 altered proteins in the epilepsy hippocampus, neuronal proteins were significantly enriched (Fisher's exact test,  $P = 6.49 \times 10^{-7}$ ),

particularly excitatory neuron proteins ( $P = 7.128 \times 10^{-6}$ ) (Fig. 4A). There was no enrichment of inhibitory neuronal, oligodendroglial, astrocytic, microglial or endothelial proteins (Fig. 4A). These enrichments were not observed in the frontal cortex (Fig. 4B), suggesting more extensive protein alterations in hippocampal neurons. All neuron-specific proteins ('neuron', 'inhibitory neuron' or 'excitatory neuron' proteins) were predominantly decreased in the epileptic hippocampus compared with controls (Fisher's exact test,  $P = 0.0013$ , Fig. 4C).

Pathway analysis showed that altered hippocampal and frontal cortex proteins were significantly associated with four pathways: protein biogenesis, mitochondrial function, synaptic plasticity and G-protein signalling (Fig. 4D and E; Supplementary Tables 18 and 19). Proteins associated with EIF2 signalling were particularly enriched. Most (37/53) were ribosomal proteins and 96.9% were upregulated (19/19 in frontal cortex, 31/33 in the hippocampus), indicating increased translational machinery and ribosome biogenesis. Other proteins involved in this pathway included translation initiation factors (EIF2AK2, EIF3E, EIF3J, EIF4E, EIF4G1) and protein kinases (MAPK1, MAPK3). The mTOR signalling pathway, as well as the regulation of eIF4 and p70S6K signalling pathway—which is part of the mTORC1-S6K signalling axis—were also significantly represented, suggesting that mTOR pathway may drive this increase in proteins related to protein synthesis. The mTOR signalling pathway is involved in protein synthesis, synaptic plasticity, autophagy and other functions which may influence neuronal excitability and epileptogenesis.<sup>76,77</sup> Oxidative phosphorylation proteins were also enriched in both regions, with broader evidence of altered mitochondrial function including pathways such as mitochondrial dysfunction, sirtuin signalling, glycolysis and TCA cycle, highlighting impaired neuronal energy regulation in epilepsy. The synaptogenesis signalling pathway was also significantly enriched, confirming synaptic dysfunction resulting from epilepsy. Finally, G-protein signalling was also significantly represented in both regions (G Beta Gamma Signalling/Ephrin B signalling; Fig. 4D and E; Supplementary Tables 16 and 17). Notably, we observed a unique enrichment of glutamate receptor signalling pathway proteins in the frontal cortex and in the remodelling of epithelial adherens junction pathway in the hippocampus. Combined, these results suggest that although changes were more prominent in the hippocampus, similar pathways were enriched in frontal cortex, identifying widespread brain protein alterations in epilepsy.

## Proteomic differences in epilepsy and control cases in the dentate gyrus

Proteomic analysis of the dentate gyrus in epilepsy was limited by smaller tissue area and increased variation.

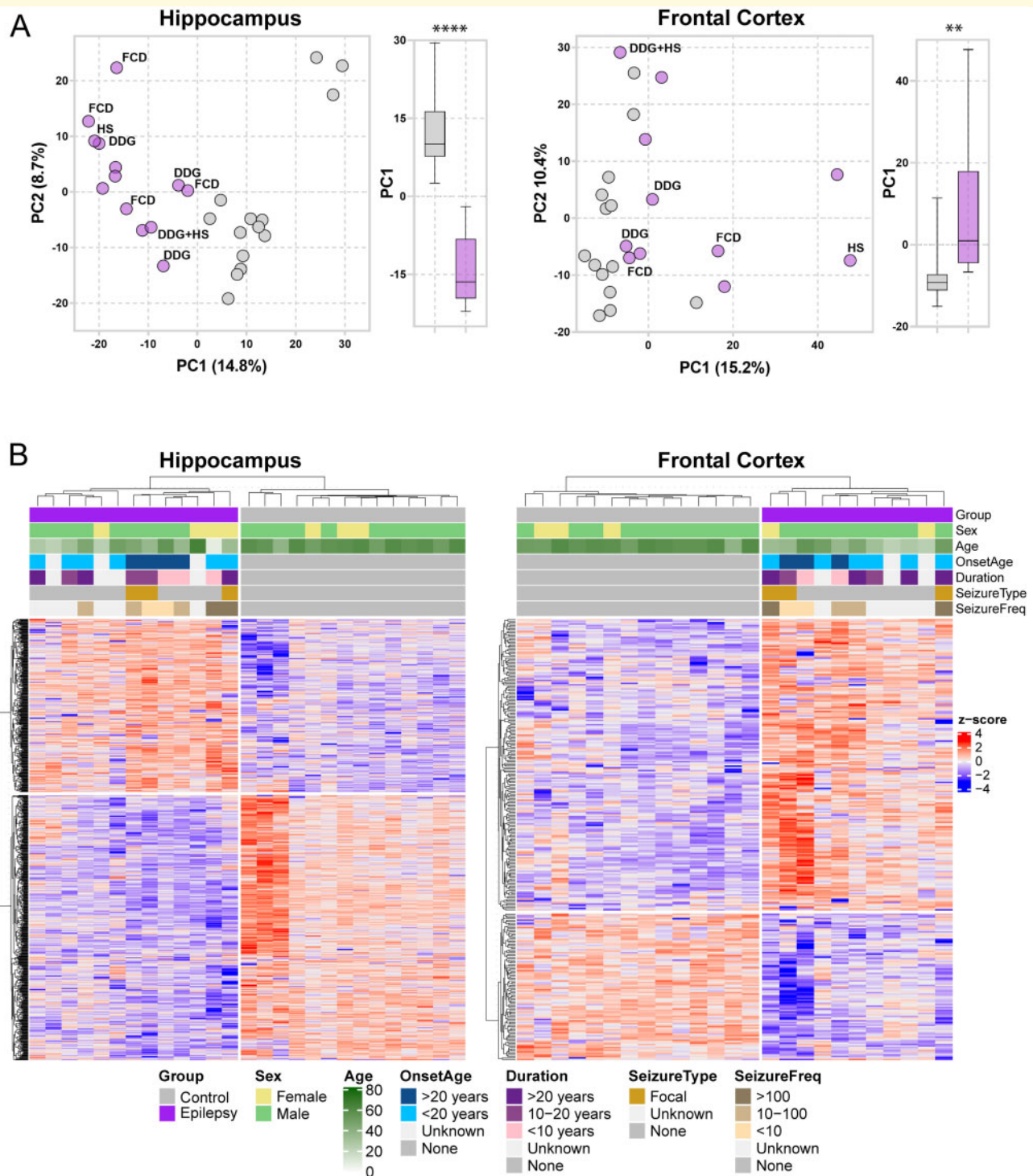


**Figure 2** Proteomic differences in epilepsy and control cases in hippocampus (CA1–3) and frontal cortex. **(A)** PCAs of overall data set for each region. PCAs of epilepsy (purple) and control (grey) cases in the hippocampus (left panel) and frontal cortex (right panel) showing that epilepsy hippocampus ( $P = 5.1 \times 10^{-5}$ ) and frontal cortex ( $P = 0.002782$ ) contained significantly different protein expression. Each point represents an individual case. Neuropathology (DDG, Dysgenesis of the Dentate Gyrus; FCD; Focal Cortical Dysplasia; HS, Hippocampal Sclerosis) is indicated on the PCA. Significance was determined using a non-parametric permutation-based  $t$ -test. Error bars represent PC1 min and max. **(B)** Supervised hierarchical clustering. Dendrogram showing hierarchical clustering of brain samples based on protein expression levels by region (left panel, hippocampus; right panel, frontal cortex). Information on diagnosis, sex, age, age of disease onset (OnsetAge), disease duration (Duration), seizure type (SeizureType), and frequency of lifetime seizures (SeizureFreq) is indicated according to the legend at the bottom of the graph. Heatmaps on the bottom show scaled (protein z-score) expression values (colour-coded according to the legend on the right) for proteins used for clustering.

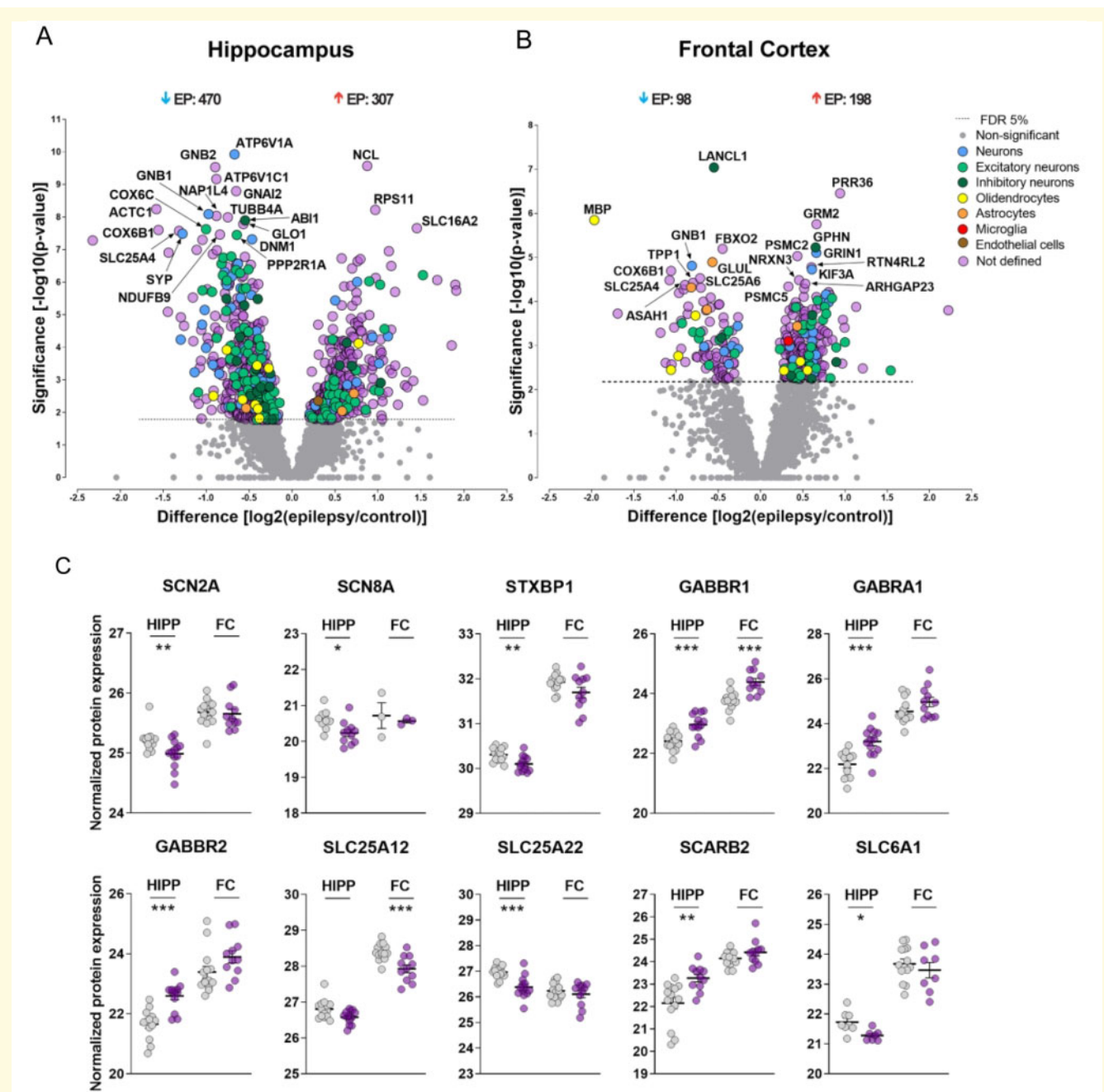


**Figure 3 Hippocampal and cortical differences in the epilepsy proteome.** Volcano plots show protein expression differences of all proteins identified in the hippocampus (**A**) and frontal cortex (**B**). All colour-coded proteins had significantly altered expression in epilepsy and are indicated above the designated line showing 5% FDR. Proteins were assigned to a specific cell-type (Neu, Neuron [blue]; In, Inhibitory Neuron [dark green]; Ex, Excitatory Neuron [light green]; Oli, Oligodendroglia [yellow]; Ast, Astrocyte [orange]; Mic, Microglia [red]; End, Endothelial cell [brown]). Significance was determined using a Student's *t*-test with Permutation based false discovery rate (FDR) set to 5% (exact *P*-values for each protein group are provided in [Supplementary Table 5](#)). Proteins with higher expression in epilepsy are on the right of the plot and proteins with lower expression are on the left. The 20 top most significantly altered proteins are identified by gene abbreviations. (**C**) Proteins of interest with significantly altered levels in epilepsy in hippocampus and frontal cortex. Individual points show protein expression in each individual case. Data show mean  $\pm$  SEM; \*\*\*\**P* < 0.0001; \*\*\**P* < 0.001; \*\**P* < 0.01. HIPP, hippocampus; FC, frontal cortex.

PCA only showed a modest separation between epilepsy and control cases ( $P = 0.246$ ) in the dentate gyrus ([Supplementary Fig. 1A](#)). However, quantification of individual proteins showed that 49 proteins were significantly

altered in the dentate gyrus in epilepsy ([Supplementary Fig. 1B](#) and [Table 11](#)). Notably, 24 proteins were uniquely altered in the dentate gyrus, including 2 identified only in dentate gyrus (CPSF1, FAM120C) and 2 identified

**Table 3 Top 20 significant proteins in the hippocampal CA1 – 3 region of epilepsy cases**

Gene ID	Protein Name	UniProt ID	P Value	Fold Change	Human	Animal Model	References
<b>Decreased</b>							
ATP6V1A	V-type proton ATPase catalytic subunit A	P38606	1.202E-10	1.591	☒	☒	46–49
GNB2	Guanine nucleotide-binding protein G(I)/G(S)/G(T) subunit beta-2	P62879	2.951E-10	1.853	☐	☒	49
ATP6V1C1	V-type proton ATPase subunit C 1	P21283	6.918E-10	1.840	☐	☒	49
GNAI2	Guanine nucleotide-binding protein G(i) subunit alpha-2	P04899	1.622E-09	1.569	☒	☒	50, 49
ACTC1	Actin, alpha cardiac muscle 1	P68032	5.754E-09	2.990	☐	☐	7, 50, 51, 52
GNB1	Guanine nucleotide-binding protein G(I)/G(S)/G(T) subunit beta-1	P62873	8.128E-09	1.959	☒	☐	7, 50, 51, 52
NAP1L4	Nucleosome assembly protein 1-like 4	Q99733	9.333E-09	1.840	☒	☒	50, 49
TUBB4B	Tubulin beta-4B chain	P68371	1.023E-08	1.682	☐	☐	49
ABI1	Abl interactor 1	Q8IZP0	1.288E-08	1.464	☐	☒	49
GLO1	Lactoylglutathione lyase	Q04760	1.66E-08	1.485	☐	☒	49
COX6C	Cytochrome c oxidase subunit 6 C	P09669	2.399E-08	2.000	☐	☐	7, 50, 49
COX6B1	Cytochrome c oxidase subunit VIb isoform 1	P14854	2.512E-08	2.949	☒	☒	7, 50, 49
SLC25A4	ADP/ATP translocase 1	P12235	2.692E-08	2.479	☒	☒	50, 49
SYN	Synaptophysin	P08247	3.236E-08	2.428	☒	☒	7, 50, 49, 53–55
NDUFB9	NADH dehydrogenase [ubiquinone] 1 beta subcomplex subunit 9	Q9Y6M9	3.467E-08	1.790	☒	☒	50, 49
PPP2R1A	Serine/threonine-protein phosphatase 2A 65 kDa regulatory subunit A alpha isoform	P30153	3.548E-08	1.558	☒	☐	7, 48
DNM1	Dynamitin-1	Q05193	4.898E-08	1.385	☒	☒	7, 49, 56, 57
<b>Increased</b>							
NCL	Nucleolin	P19338	2.692E-10	1.828	☒	☒	50, 58, 59
RPS11	40S ribosomal protein S11	P62280	6.026E-09	1.959	☐	☐	50, 49
SLC16A2	Monocarboxylate transporter 8	P36021	2.188E-08	2.732	☒	☒	50, 49

**Table 4 Top 20 significant proteins in the frontal cortex of epilepsy cases**

Gene ID	Protein Name	UniProt ID	P Value	Fold change	Human	Animal model	References
<b>Decreased</b>							
LANCL1	Glutathione S-transferase LANCL1	O43813	9.12E-08	1.464	☐	☒	49
MBP	Myelin basic protein	P02686	1.445E-06	3.891	☒	☒	49,50,60,61
FBXO2	F-box only protein 2	Q9UK22	6.457E-06	1.366	☒	☒	48–50
GLUL	Glutamine synthetase	P15104	1.288E-05	1.485	☒	☒	7, 48, 62, 64
GNB1	Guanine nucleotide-binding protein G(I)/G(S)/G(T) subunit beta-1	P62873	1.549E-05	1.753	☒	☐	7, 50, 52
COX6B1	Cytochrome c oxidase subunit 6B1	P14854	2.042E-05	2.085	☒	☒	7, 49, 50
SLC25A6	ADP/ATP translocase 3	P12236	2.951E-05	1.636	☐	☐	49, 50
SLC25A4	ADP/ATP translocase 1	P12235	3.311E-05	2.114	☒	☒	49, 50
TPPI	Tripeptidyl-peptidase 1	O14773	3.802E-05	1.741	☒	☒	7, 49, 50
ASAH1	Acid ceramidase	Q13510	4.169E-05	1.853	☒	☒	7, 48–50, 65
<b>Increased</b>							
PRR36	Proline-rich protein 36	Q9H6K5	3.548E-07	1.919	☐	☐	66–69
GRM2	Metabotropic glutamate receptor 2	Q14416	1.778E-06	1.580	☒	☒	7, 70–73
GPHN	Gephyrin	Q9NQX3	5.888E-06	1.569	☒	☒	7, 49, 74
GRIN1	Glutamate receptor ionotropic, NMDA 1	Q05586	7.943E-06	1.580	☒	☒	7, 49, 74
PSMC2	26S proteasome regulatory subunit 7	P35998	9.333E-06	1.347	☐	☐	50
RTN4RL2	Reticulon-4 receptor-like 2	Q7M6Z0	1.66E-05	1.516	☐	☐	50
KIF3A	Kinesin-like protein KIF3A	Q9Y496	1.862E-05	1.526	☒	☐	75
NRXN3	Neurexin-3-beta	Q9HDB5	3.311E-05	1.366	☒	☐	49
ARHGAP23	Rho GTPase Activating Protein 23	Q9P227	3.981E-05	1.444	☐	☒	50
PSMC5	26S proteasome regulatory subunit 8	P62195	4.571E-05	1.257	☒	☐	50

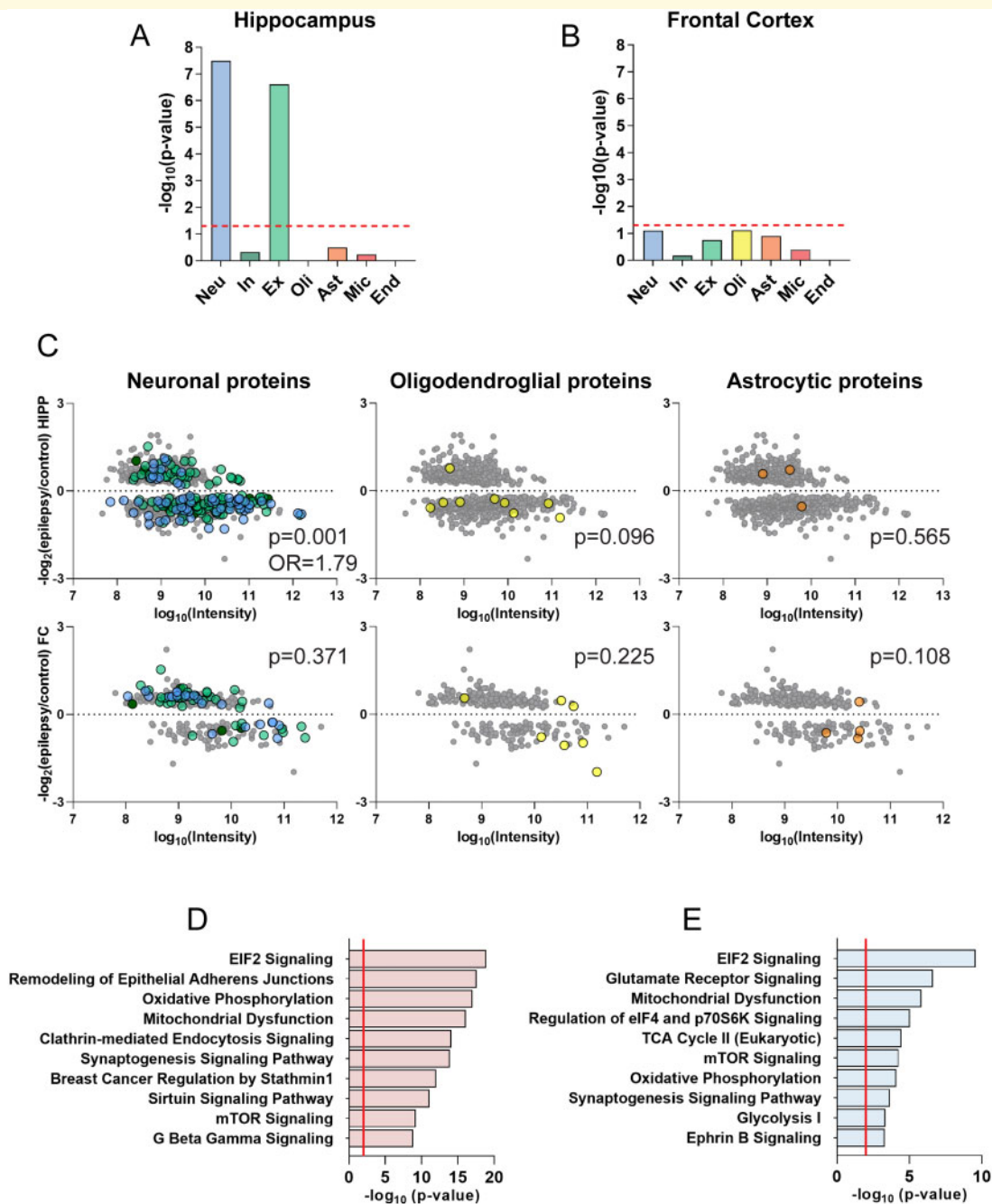


**Figure 4 Cell-type enrichment and pathway analysis of differentially expressed proteins in the hippocampus and frontal cortex in epilepsy.** For each brain region [Hippocampus (A), frontal cortex (B)], cell-type enrichment analysis was performed for each cell type using a Fisher's exact test. Significance threshold is represented by a dotted red line ( $P < 0.05$ ); \*\*\*\* $P < 0.0001$ . (C) Cell-type-specific protein expression differences in epilepsy. Each graph plots all significant proteins quantified in the epilepsy hippocampus (top panels) or frontal cortex (bottom panels). The further the point is away from the dashed line at 0, the greater the difference in expression in epilepsy and controls. Proteins with a positive log ratio have greater expression in epilepsy, and proteins with a negative log ratio have a lower expression in epilepsy. All color-coded proteins correspond to neuronal proteins (Neuron, blue; Inhibitory Neuron, dark green; Excitatory Neuron, dark green), oligodendrocyte proteins (yellow) and astrocyte proteins (orange). The cumulative cell type specific protein expression differences showed that there were significantly less neuronal proteins in the hippocampus in epilepsy ( $P = 0.001$ ) but not in the frontal cortex ( $P = 0.371$ ). No differences in the amount of oligodendroglial (hippocampus,  $P = 0.096$ ; frontal cortex,  $P = 1$ ), astrocytic (hippocampus,  $P = 0.565$ ; frontal cortex,  $P = 0.108$ ), microglial (not shown) or endothelial proteins (data not shown) were observed. Significance was determined using a Fisher's exact test comparing cumulative cell type specific protein expression between epilepsy and control cases. Pathway analysis of the altered proteome in the hippocampus (D) and frontal cortex (E). IPA was used to identify the top 10 signalling pathways associated with the genes encoding protein groups that were significantly altered in both the hippocampus (pink) and the frontal cortex (blue). The red line corresponds to FDR corrected  $P$ -value thresholds (hippocampus,  $P = 0.0001$ ; frontal cortex,  $P = 0.001$ ). All pathways and proteins are shown in [Supplementary Tables 16 and 15](#).

only in dentate gyrus and frontal cortex (CDC5L, AMER2) (Supplementary Table 5). Hierarchical clustering induced by pre-selection of these differently expressed proteins showed that 10/13 epilepsy cases clustered, supporting dentate gyrus dysfunction in epilepsy (Supplementary Fig. 1C). Supplementary Table 3 lists the 20 most significantly altered proteins; 16 (80%) are associated with epilepsy in humans or animal models, while 4 (20%) were novel (AMER2, ATP5BP, RPL15, TPI1), adding to the list of potential new epilepsy-associated proteins (Tables 3 and 4; Supplementary Tables 1 and 2). The G-Protein Subunit Beta 1 (GNB1) was the only protein to rank among the top 20 significantly altered proteins in all regions (hippocampus,  $P = 8.19 \times 10^{-9}$ ; frontal cortex;  $P = 1.55 \times 10^{-5}$ , dentate gyrus;  $P = 6.96 \times 10^{-6}$ ; Supplementary Fig. 1D). Despite the epileptic encephalopathies that *GNB1* mutations can cause,<sup>78</sup> the underlying disease mechanisms are still largely unknown and the specific role of *GNB1* in epileptogenesis has not yet been studied. Pathway analysis of altered proteins in the dentate gyrus showed the most enrichment in proteins involved in mitochondrial dysfunction, revealing a common epilepsy proteomic signature in all regions (Supplementary Fig. 1E and Table 18).

### Inter-regional epilepsy proteomic signature

The common enriched pathways in the hippocampus and frontal cortex (Fig. 4D and E), as well as the overlapping altered proteins (Fig. 5A), indicate shared protein changes across both regions. We performed correlation analyses of the directional changes in hippocampus and frontal cortex for the (i) 939 significantly altered proteins and (ii) 134 common proteins altered in both regions (Fig. 5B and C; Supplementary Table 13). We found a modest positive correlation between protein levels in the hippocampus and frontal cortex when all significant proteins were examined (Pearson's correlation,  $r^2=0.32$ , Fig. 5B), suggesting that the hippocampus was more severely and/or differently impacted compared with the frontal cortex. The correlation improved when analysing the changes of the 134 significantly different proteins shared by both the hippocampus and frontal cortex ( $r^2=0.73$ , Fig. 5C), confirming broad similar protein alterations throughout the epileptic brain. Interestingly, this correlation was also present in the dentate gyrus (hippocampus/dentate gyrus,  $r^2=0.64$ ; frontal cortex/dentate gyrus,  $r^2=0.72$ , Fig. 5D and E), despite only 13/134 of these proteins being significantly altered in the dentate gyrus (Fig. 5A, D and E; Supplementary Table 13), supporting an epilepsy-associated proteomic signature. Hierarchical clustering of these specific proteins shows almost complete clustering of all epilepsy cases throughout the three regions analysed (Fig. 5F). These 134 enriched proteins relate to EIF2 and mTOR signalling pathways, mitochondrial dysfunction and other related metabolic pathways such as oxidative

phosphorylation, glycolysis, TCA cycle and gluconeogenesis (Fig. 6A and B; Supplementary Table 19). Proteins involved in G-protein signalling were also significantly enriched (Ephrin B signalling; Fig. 6A and B; Supplementary Table 19).

Together, these results support a broad impact of epilepsy on mitochondrial function, protein biogenesis and G-protein signalling. Notably, synaptic plasticity-related signalling pathways were not among shared significant proteins changes across hippocampus and frontal cortex, suggesting that the synaptic-associated mechanisms differ between these regions.

### Intra-regional epilepsy proteomic changes

We found that 635 proteins reached significance in the hippocampus and not in the frontal cortex. These highly significant hippocampal differences were enriched in proteins involved in the remodelling of epithelial junction ( $P = 7.71 \times 10^{-18}$ ), with prominent involvement of cytoskeleton-associated proteins (actin-related [ACTC1, ACTG1, ACTN1, ACTR2, ACTR3, ARPC4, ARPC1A], dynamins [DNM1, DNM2, DNM3, DNM1L] and tubulins [TUBA1A, TUBA1B, TUBA4A, TUBB3, TUBB, TUBB2A, TUBB4A]) and clathrin-mediated endocytosis signalling ( $P = 7.92 \times 10^{-16}$ ), suggesting a reorganization of the cortical microarchitecture and a remodelling of neuronal circuitries, or an impact on the brain vasculature (Supplementary Table 20). A significant alteration in synaptogenesis signalling pathway proteins was also observed ( $P = 6.26 \times 10^{-14}$ ; Supplementary Table 20). These findings, together with the significant decrease of neuronal proteins observed previously (Fig. 4C) suggest neuronal synaptic dysfunction in the hippocampus. Neuronal loss is another possible explanation but was not seen histologically. Using a publicly available data set of the most updated synaptic proteome,<sup>43</sup> we confirmed that the significant proteins in the hippocampus were highly enriched in neuro-synaptic proteins (33/63 neuro-synaptic proteins, Fisher's exact test,  $P = 3.939 \times 10^{-6}$ ; Supplementary Table 7). The expression of significant synaptic proteins in epilepsy was dramatically decreased (55/58 proteins, Fisher's exact test,  $8.133 \times 10^{-10}$ , Fig. 7A), suggesting extensive synaptic alteration in the hippocampus. These proteomic changes were not significant in the frontal cortex (Fisher's exact test,  $P = 0.089$ ; Fig. 7B; Supplementary Table 7). We validated the decrease of SYP in the epileptic hippocampus using IHC (Fig. 7C, E and G). To determine whether these protein changes were unique to this region or simply less pronounced in the frontal cortex than in the hippocampus, we examined the directional changes of the significantly altered hippocampal proteins and their respective directional change in the frontal cortex. When we closely examined these differences, we discovered that the vast majority of these proteins were showing trends for similar changes in the frontal cortex

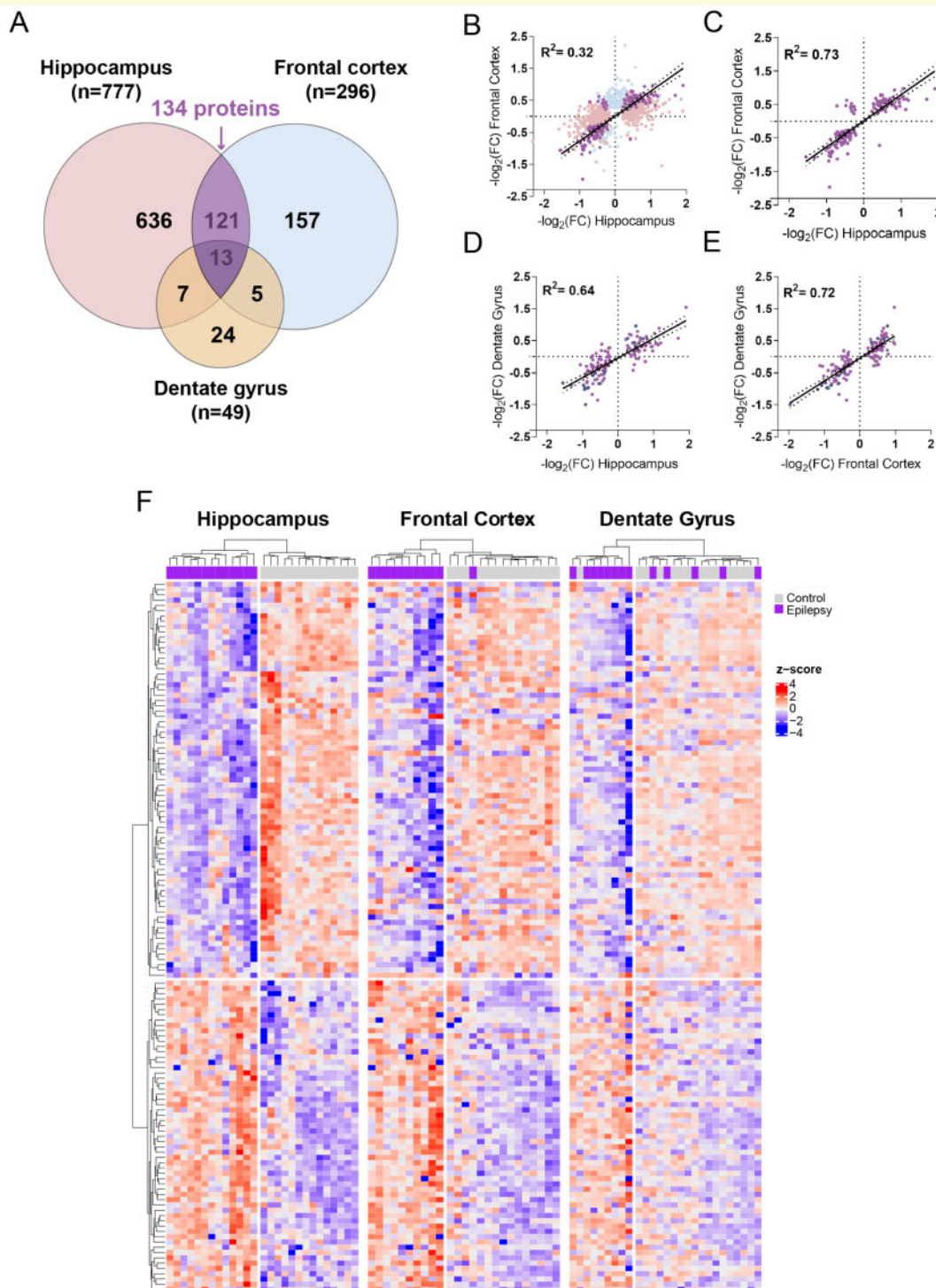


**Figure 5 Inter-regional epilepsy proteomic signature.** (A) Venn diagram of significant proteins in each region. The Venn diagram shows the 963 altered proteins in epilepsy across all regions analysed. A total of 939 proteins were altered in hippocampus and frontal cortex altogether. There were 134 overlapping proteins between the hippocampus and the frontal cortex (purple), and 13 overlapping proteins across the three regions (dark blue). (B–E) Correlation between the protein fold changes in the hippocampus and the frontal cortex. Graphs represent correlations using the 939 significantly altered proteins (top left panel, Pearson's correlation,  $r^2=0.32$ ), and the overlapping 134 proteins altered in both hippocampus and frontal cortex [top right panel, Pearson's correlation ( $r^2=0.73$ )]. The proteomic signature was also preserved in the dentate gyrus, despite only 13/134 proteins being significant [bottom panels, Pearson's correlation; hippocampus/dentate gyrus (bottom left panel),  $r^2=0.64$ ; frontal cortex/dentate gyrus (bottom right panel),  $r^2=0.72$ ]. (F) Hierarchical clustering of the 134 proteins showing similar directional changes in hippocampus CA1–3, frontal cortex and dentate gyrus. The dendrogram shows hierarchical clustering of brain samples based on protein expression levels by region. The heatmap on the bottom show scaled (protein z-score) expression values (color-coded according to the legend on the right) for proteins used for clustering.

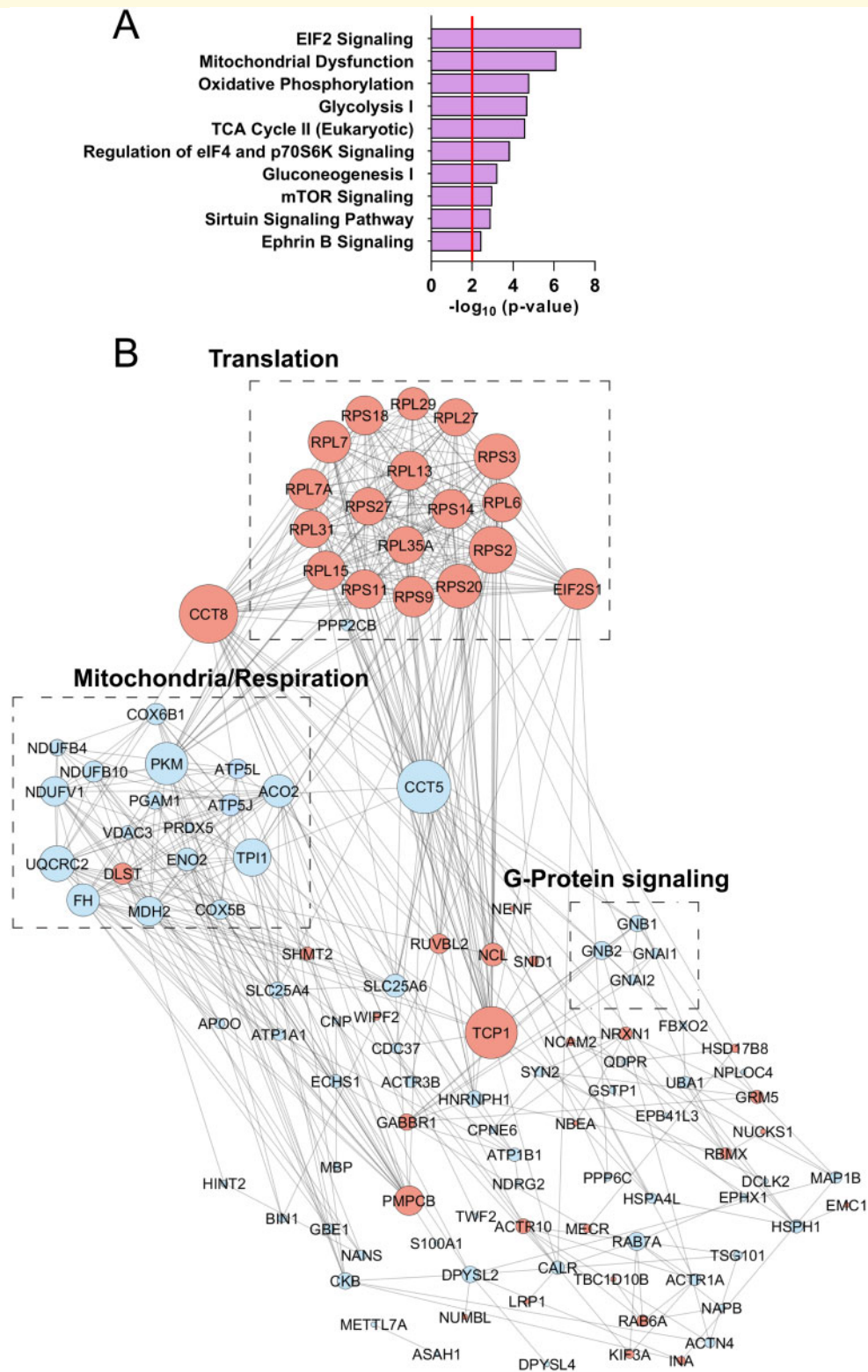


**Figure 6 Pathway and network analysis of the epilepsy proteomic signature.** (A) Pathway analysis of the epilepsy proteomic signature. IPA was performed on genes encoding for protein groups significantly altered in the proteomic signature. The red line corresponds to FDR corrected  $P$ -value threshold ( $P = 0.05$ ). (B) Epilepsy proteomic signature protein network. The network depicts altered proteins in both hippocampus and frontal cortex. Visualization and analysis of the network was conducted via Cytoscape. Color-coding represents directional changes (upregulated shown in red, downregulated shown in blue). Node sizes correspond to degree of interaction. Disconnected nodes in the network were removed. Black rectangles correspond to proteins involved in pathways of interest.



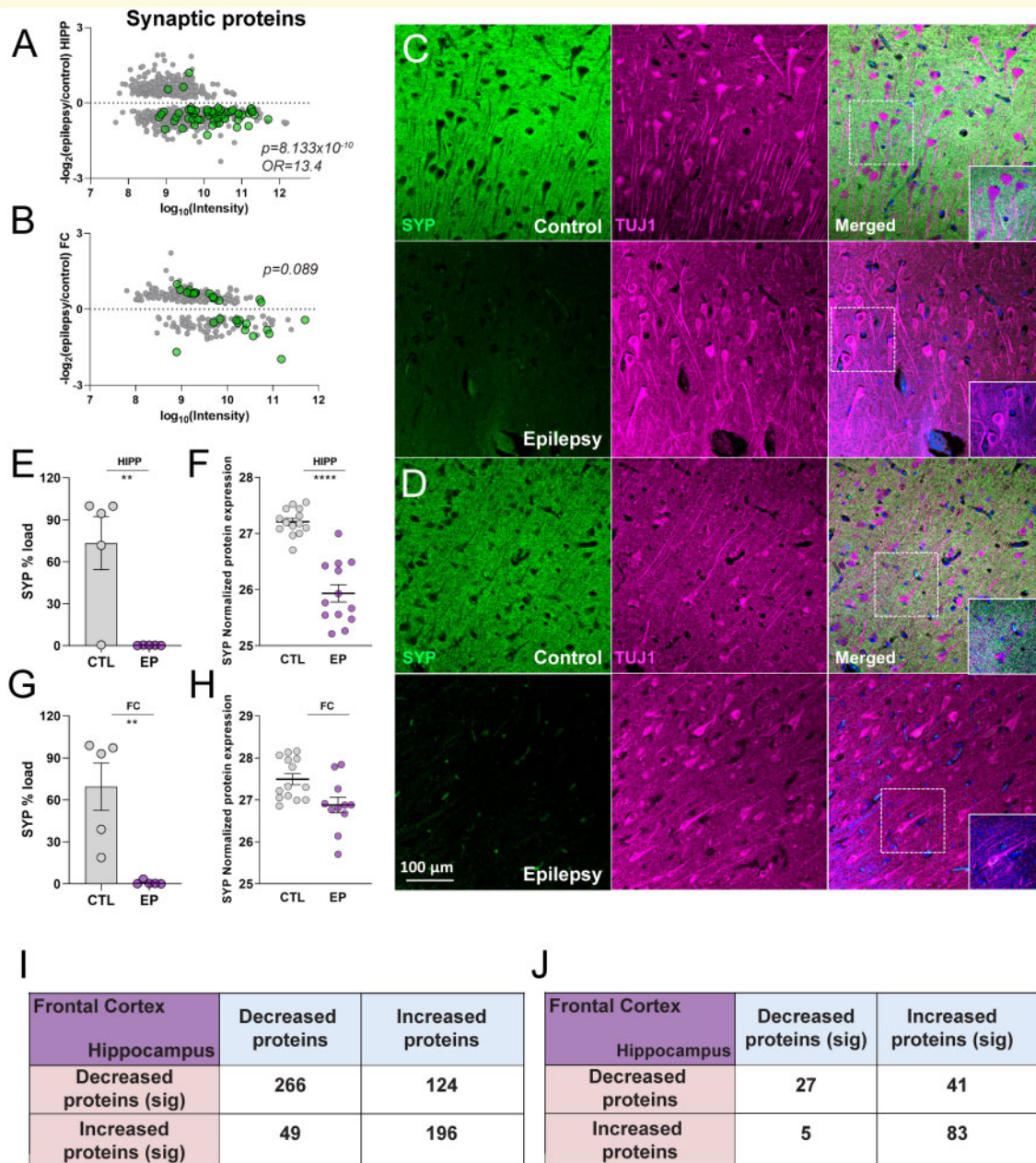


**Figure 7 Altered synaptic transmission in epilepsy.** (A) The graph depicts all significant proteins identified in the hippocampus. The further the point is away from the dashed line at 0, the greater the difference in expression in epilepsy and controls. Proteins with a positive log ratio have greater expression in epilepsy and proteins with a negative log ratio have a greater expression in controls. All proteins highlighted in green correspond to synaptic proteins. (B) The graph shows all significant proteins identified in the frontal cortex. All proteins highlighted in green correspond to synaptic proteins. (C) Synaptophysin (SYP) and Tubulin- $\beta$  3 (TUJ1) double fluorescent immunohistochemistry of  $n = 5$  epilepsy and  $n = 5$  control cases in the hippocampus showed a major decrease in SYP immunoreactivity in the epileptic hippocampus [panels show CA1 region, images taken at  $\times 20$  (top panels) and  $\times 63$  magnification (bottom panels)]. (D) SYP and TUJ1 double fluorescent immunohistochemistry of  $n = 5$  epilepsy and  $n = 5$  control cases in the frontal cortex also showing major decrease in SYP immunoreactivity in the epileptic cortex [images taken at  $\times 20$  (top panels) and  $\times 63$  magnification (bottom panels)]. (E–H) Quantification of SYP immunohistochemistry (E–G) and proteomic expression levels (F–H) in the hippocampus CA1–3 (E, F) and frontal cortex (G, H) ( $n = 5$ /group for IHC and  $n = 14$ /group for proteomics) epilepsy. For IHC quantification, individual points show SYP % load in each individual case (E–G). Significance was determined using a two-tailed unpaired  $t$ -test. Data show mean  $\pm$  SD;  $**P < 0.01$ . For proteomics, individual points show protein expression in each individual case (F–H). Data show mean  $\pm$  SEM;  $****P < 0.0001$ . HIPP, hippocampus; FC, frontal cortex. (I, J) Topographical changes in epilepsy support the idea of selective vulnerability in hippocampus. The left panel shows a contingency table of the protein directional changes between epilepsy and control in the hippocampus and frontal cortex using the significant proteins in hippocampus only. The right panel shows a contingency table of the protein directional changes between epilepsy and control in the hippocampus and frontal cortex using the significant proteins in frontal cortex only. Proteins were annotated as either increased or decreased in epilepsy. Only proteins present in both regions were included in the analysis. Significance was determined using Fisher's exact test.

(462/635 proteins in agreement [72%], Fisher's exact test,  $P < 2.2 \times 10^{-16}$ , Fig. 7I), suggesting that overall the same pathological protein changes were happening in the frontal cortex, but not to the same extent. IPA confirmed that the proteins that were in agreement were involved in the remodelling of epithelial adherens junctions ( $P = 2.14 \times 10^{-12}$ ), and synaptogenesis ( $P = 1.52 \times 10^{-10}$ ). The significantly decreased SYP immunoreactivity in the frontal cortex also supported this observation (Fig. 7D, F and H).

Similarly, we found that 156 proteins reached significance in the frontal cortex and not in the hippocampus. While these frontal cortex protein changes were also suggestive of altered synaptogenesis, these changes were mostly enriched in proteins involved in increased glutamate receptor signalling (8/57 proteins,  $P = 2.61 \times 10^{-7}$ ,  $z$ -score = 2.236; Supplementary Table 21), which occurs in glutamatergic synapses, and plays a critical role in excitotoxic damage in epilepsy.<sup>79</sup> Proteins in this pathway included protein Glutamine Synthetase (GLUL), Excitatory amino acid transporters 1 and 2 (SLC1A2, SLC1A3), Glutamate receptor ionotropic NMDA 1 and 2B (GRIN1, GRIN2B), Glutamate receptor ionotropic AMPA 2 (GRIA2) and Glutamate metabotropic receptor 2 (GRM2). Interestingly, GLUL downregulation was associated with reduced astrocyte protection against glutamate excitotoxicity to neurons.<sup>80</sup> Here again, we found that the majority of these significant changes which seemed specific to the frontal cortex were showing trends for similar directional changes in the hippocampus (110/156 proteins in agreement [72%],  $P = 1.753 \times 10^{-7}$ , Fig. 7J), suggesting that most of these changes were also occurring in the hippocampus, yet to a lesser extent. IPA confirmed that the proteins in agreement were most enriched in the glutamatergic signalling pathway ( $P = 7.58 \times 10^{-5}$ ).

Combined, our results indicate that 696/939 (74%) significant proteins had similar directional changes in both the hippocampus and frontal cortex in epilepsy (Supplementary Table 21). These findings suggest that most pathological protein changes in epilepsy occurred in both regions but to a different degree, supporting greater vulnerability or a primary role of the hippocampus compared with the frontal cortex.

## Discussion

In this study, we have generated the first comprehensive characterization of the human epileptic proteome. We identified extensive protein alterations common to various epilepsy syndromes in multiple brain regions. The epileptic hippocampus and frontal cortex showed dysregulation in pathways associated with mitochondrial function, protein synthesis, synaptic transmission and remodelling of the neuronal network architecture. These protein alterations were present despite the lack of major

neurodegeneration. Our proteomics analysis provides a network-level analysis of protein changes in epilepsy and identifies hundreds of new potential drug targets. Given the paucity of comprehensive proteomics studies, it was difficult to cross-validate our findings. However, Wang et al. presented the most updated summary of the genes associated with epilepsy, grouping these genes according to the manifestation of epilepsy in specific phenotypes. We compared our list of 939 altered proteins (hippocampus and frontal cortex) with this list and found that 20/939 proteins were encoded by genes in which mutations cause epilepsy.<sup>7</sup> Importantly, 98/939 proteins were encoded by neurodevelopment-associated epilepsy genes, epilepsy-related genes, or potentially epilepsy-associated genes. In addition, we compared the top 20 most significant proteins in each region with the few other human and animal studies available. While there were some differences compared with previous literature, the majority of the proteins in Supplementary Tables 1–3 had similar directional changes to those previously reported. However, some of these discrepancies may be related to the evaluation of various epilepsies, brain regions and techniques. Our results also suggest that the G-protein heterotrimeric complexes may have a particularly important role in epilepsy and specifically highlighted the widespread decrease in GNB1 expression levels in epilepsy.

Our results showed that the hippocampus was particularly vulnerable in epilepsy and suggested that protein changes in epilepsy may progressively extend through the brain in a topographic manner. The increased vulnerability of the hippocampus was evident in the broad range of epilepsy syndromes included in this study. The hippocampus is an epileptogenic brain region that is highly susceptible to damage from seizures. As a result, hippocampal sclerosis is a common neuropathological feature of epilepsy and its incidence varies from 30 to 45% of all epilepsy syndromes and 56% of MTLT neuropathologically.<sup>81</sup> Hippocampal sclerosis is the most common pathology associated with drug-resistant epilepsy in older adults.<sup>82</sup> Our cohort only included two cases with hippocampal sclerosis, which alone was not enough to explain such extensive hippocampal neuronal alterations. In contrast to earlier studies, we included a heterogeneous case cohort to identify protein alterations across a spectrum of epilepsy syndromes. Our study suggests that hippocampal vulnerability is a consistent feature across all types of epilepsy. It remains unknown why the hippocampus is so vulnerable in epilepsy as well as in ischaemia, limbic encephalitis, multiple sclerosis, and neurodegenerative diseases such as Alzheimer's disease.<sup>83–87</sup> The cognitive deficits in temporal lobe epilepsy are associated with Alzheimer-like amyloid  $\beta$  and tau protein changes.<sup>88</sup> Hippocampus vulnerability in epilepsy and other neurological disorders may result from a low threshold for glutamatergic excitotoxicity or for synaptic remodelling. Some studies show vulnerability correlates with increased neuroplasticity, which could reflect different energy

production mechanisms and requirements, making it highly sensitive to metabolic and oxidative stress, which can occur in epilepsy.<sup>89</sup>

Our results suggest that epilepsy affects brain areas in parallel yet to a different degree, supporting that epilepsy may be a progressive disease.<sup>90</sup> Hippocampal protein alterations reflected pathologic changes of degeneration, such as neuronal and synaptic remodelling, which were also observed in the frontal cortex without reaching a significant threshold of 5% FDR (Supplementary Fig. 2). While decreased synaptophysin immunoreactivity was found in temporal lobe epilepsy-associated HS,<sup>91</sup> our study is the first to report significantly decreased synaptophysin levels in epilepsy cases in the frontal cortex and hippocampus without hippocampal sclerosis. In contrast, frontal cortex protein changes seemed to mainly reflect earlier pathological changes such as an altered glutamatergic system, with non-significant but similar directional changes in the hippocampus. However, both regions showed mitochondrial dysfunction and altered protein synthesis, although these changes were more prominent in the hippocampus (Supplementary Fig. 2). The shared regional changes in mitochondrial function and protein biosynthesis, as well as the more localized frontal changes in the glutamatergic system suggest that these may be relatively earlier events in the disease process. The lack of significant glutamatergic changes in the hippocampus may reflect the statistical noise of the large protein changes, or that as the disease progresses, these neurons may be selectively lost or compensatory changes wash out any effect. Glutamatergic hyperactivity may be an early insult, driving or resulting from epileptic activity, and leading to oxidative stress and mitochondrial dysfunction; although, this remains unproven. Mitochondrial dysfunction lowers intracellular levels of ATP and alters calcium homeostasis, and these two pathways may be linked in a feed-forward pathologic cycle.<sup>92</sup> Whether mitochondrial dysfunction is a cause or a consequence of epilepsy—or both—our study shows it is a widespread change in the epilepsy brain. Many metabolic and mitochondrial disorders cause seizures and disorders such as myoclonic epilepsy with ragged red fibres.<sup>93,94</sup> Seizures occur in 35–60% of individuals with primary mitochondrial diseases.<sup>95</sup> Mitochondrial oxidative stress occurs in temporal lobe epilepsy,<sup>96–98</sup> but it remains uncertain if this is part of epileptogenesis or a secondary effect of seizures, ASDs or other factors. Mitochondrial functions can affect neuronal hyperexcitability via generation of ATP, metabolite/neurotransmitter biosynthesis, calcium homeostasis, reactive oxygen species production and apoptosis. Our study suggests that mitochondrial dysfunction may both contribute to and result from epilepsy. Our study also identified significantly increased protein biosynthesis in epilepsy. While this increase could be a result of loss of neuronal homeostasis due to mitochondrial dysfunction,<sup>99</sup> increased protein synthesis may be driven by altered mTOR signalling, which was a prominent finding in our results. mTOR signalling pathways are implicated in a

number of epileptogenic processes.<sup>100</sup> Our results suggest increased ribosome biogenesis and protein production in chronic epilepsy. Protein synthesis may shift towards greater production of both pro-epileptic factors and compensatory anti-epileptic factors.<sup>101</sup> Also, dysregulated mTOR signalling, part of the proteomic signature of epilepsy, may stimulate excessive synthesis of ion channels and receptors, leading to hyperexcitability.<sup>102</sup>

Our findings identified significant G-protein subunit alterations in epilepsy (Supplementary Fig. 2). Specifically, we detected 20 protein G-subunits in our study, with 13 of them being differentially expressed in at least one region (GNG7, GNAO1, GNG2, GNG4, GNB1, GNB2, GNAI1, GNAI2, GNAQ, GNAZ, GNB4, GNA11 and GNL1). Heterotrimeric G-proteins consist of two functional units, an  $\alpha$ -subunit ( $G\alpha$ ) and a tightly associated  $\beta\gamma$  complex. After activation, GPCRs change their conformation and transduce this into intracellular signals involved in diverse signalling pathways including the cAMP/PKA pathway, calcium/protein kinase C (PKC) pathway, IP3/DAG/phospholipase C pathway,  $\beta$ -arrestin pathway, protein tyrosine kinase pathway, ERK/MAPK pathway, PI3K/AKT pathway, Rho pathway and G-protein-gated calcium channels inwardly rectifying potassium channels.<sup>103</sup> Animal studies suggest that GPCRs are important mediators of neuronal excitability, supporting a potential therapeutic role in epilepsy.<sup>104</sup> However, no FDA-approved ASD suppresses epileptic seizures by directly acting on GPCRs. GNB1 may be central to GPCR dysfunction in epilepsy.<sup>104</sup> We found that one G-protein subunit, GNB1, was significantly decreased in all the regions. Missense, splice-site and frameshift variants in the *GNB1* gene are associated with multiple neurological phenotypes, including seizures in most cases.<sup>51,52,105–108</sup> Mice harbouring the *GNB1* K78R human pathogenic recapitulate many clinical features, including developmental delay, motor and cognitive deficits, and absence-like generalized seizures, and that cellular models displayed extended bursts of firing followed by extensive recovery periods.<sup>109</sup> Given the therapeutic potential of targeting G-proteins, and the novelty of our finding, it would be interesting to further investigate the role of GNB1 in epilepsy. The involvement of *GNB1* variants in human epilepsies and our data suggest this gene may play an important role in many epilepsies. Among the 134 currently available drugs targeting GPCRs,<sup>110</sup> there are several drugs targeting GPCRs involved in pathways significantly impacted in our epilepsy data set. GNB1 is involved in 28 pathways that are significantly impacted in the hippocampus of epilepsy cases (27 inhibited, 1 activated), and 15 of these pathways include GPCRs with an FDA approved drug for non-epilepsy related indications. Future studies should evaluate whether any of these drugs or novel derivatives may be useful in ameliorating seizures in specific epilepsy syndromes. This may especially be of interest for the CREB signalling in neurons and endocannabinoid developing neuron pathways that were

significantly decreased in our data set, as well as drugs targeting GPCRs that have been specifically identified as affected in some epilepsy syndromes like ADRA2 in the adrenergic signalling pathway<sup>7</sup> in addition to glutamatergic and GABAergic targets.

Our study provides a rich resource for epilepsy research, adding to a recent transcriptomic analysis of human MTLTLE brain.<sup>50</sup> Combining different ‘-omics’ may provide complimentary facets to a more comprehensive understanding of epilepsy pathogenesis and help identify novel therapeutic targets. A limitation of this study is the heterogeneity of our cohort with diverse epilepsies, therapies and genetic backgrounds. However, our study was designed to identify common protein changes in epilepsy across heterogeneous cases, which increased variation, making the robust protein changes we observed more significant. Future studies should examine specific epilepsy syndromes as well as the role of ASDs. Our study was not powered to assess the impact of treatments, which could bias this study by altering protein levels and altering non-epilepsy pathways. For example, altered GABAergic receptors or mitochondrial function could reflect ASDs such as clobazam, clonazepam or valproic acid.<sup>111</sup>

In conclusion, our study is the first comprehensive proteomic study in the human epilepsy brain and identifies novel proteins in critical pathways that may be considered as potential drug targets. These pathways mainly include protein biogenesis, mitochondrial function, and synaptogenesis signalling. Combined, our findings provide a valuable resource for epilepsy research.

## Supplementary material

Supplementary material is available at *Brain Communications* online.

## Funding

This work was supported by Finding a Cure for Epilepsy and Seizures and the National Institute of Health grants U01NS090415, 1R1AG058267, P30AG066512 and P01AG060882. This work was supported by funding from the Bluesand Foundation to ED, Philippe Chatrier Foundation to G.P. The proteomics work was in part supported by the New York University School of Medicine and a shared instrumentation grant from the National Institute of Health, 1S10OD010582-01A1 for the purchase of an Orbitrap Fusion Lumos.

## Competing interests

The authors report no competing interests.

## References

- Ngugi AK, Bottomley C, Kleinschmidt I, Sander JW, Newton CR. Estimation of the burden of active and life-time epilepsy: a meta-analytic approach. *Epilepsia*. 2010;51(5):883–890.
- Aronica E, Mühlebner A. Neuropathology of epilepsy. *Handb Clin Neurol*. 2017;145:193–216.
- Engel J. Epileptogenesis, traumatic brain injury, and biomarkers. *Neurobiol Dis*. 2019;123:3–7.
- Thijs RD, Surges R, O'Brien TJ, Sander JW. Epilepsy in adults. *Lancet (London, England)*. 2019;393(10172):689–701.
- Halvorsen M, Petrovski S, Shellhaas R, et al. Mosaic mutations in early-onset genetic diseases. *Genet Med*. 2016;18(7):746–749.
- Scheffer IE, Berkovic S, Capovilla G, et al. ILAE classification of the epilepsies: position paper of the ILAE Commission for Classification and Terminology. *Epilepsia*. 2017;58(4):512–521.
- Wang J, Lin ZJ, Liu L, et al. Epilepsy-associated genes. *Seizure*. 2017;44:11–20.
- D’Gama AM, Walsh CA. Somatic mosaicism and neurodevelopmental disease. *Nat Neurosci*. 2018;21(11):1504–1514.
- Dunn P, Albury CL, Maksemous N, et al. Next generation sequencing methods for diagnosis of epilepsy syndromes. *Front Genet*. 2018;9:20.
- Staley K. Molecular mechanisms of epilepsy. *Nat Neurosci*. Mar. 2015;18(3):367–372.
- Hesdorffer DC, Crandall LA, Friedman D, Devinsky O. Sudden unexplained death in childhood: a comparison of cases with and without a febrile seizure history. *Epilepsia*. 2015;56(8):1294–1300.
- Devinsky O, Hesdorffer DC, Thurman DJ, Lhatoo S, Richerson G. Sudden unexpected death in epilepsy: epidemiology, mechanisms, and prevention. *Lancet Neurol*. 2016;15(10):1075–1088.
- Blumcke I, Thom M, Aronica E, et al. The clinicopathologic spectrum of focal cortical dysplasias: a consensus classification proposed by an ad hoc Task Force of the ILAE Diagnostic Methods Commission. *Epilepsia*. 2011;52(1):158–174.
- Kandratavicius L, Balista PA, Lopes-Aguiar C, et al. Animal models of epilepsy: use and limitations. *Neuropsychiatr Dis Treat*. 2014;10:1693–1705.
- Wong M, Roper SN. Genetic animal models of malformations of cortical development and epilepsy. *J Neurosci Methods*. 2016; 260:73–82.
- Reyes-Garcia SZ, Scorza CA, Araújo NS, et al. Different patterns of epileptiform-like activity are generated in the sclerotic hippocampus from patients with drug-resistant temporal lobe epilepsy. *Sci Rep*. 2018;8(1):7116
- Fukata Y, Fukata M. Epilepsy and synaptic proteins. *Curr Opin Neurobiol*. 2017;45:1–8.
- Mahoney JM, Mills JD, Mühlebner A, et al. 2017 WONOEP appraisal: studying epilepsy as a network disease using systems biology approaches. *Epilepsia*. 2019;60(6):1045–1053.
- Genetic determinants of common epilepsies: a meta-analysis of genome-wide association studies. *Lancet Neurol*. 2014;13(9): 893–903.
- Miller-Delaney SF, Bryan K, Das S, et al. Differential DNA methylation profiles of coding and non-coding genes define hippocampal sclerosis in human temporal lobe epilepsy. *Brain*. 2015;138(Pt 3):616–631.
- Dębski KJ, Pitkanen A, Puhakka N, et al. Etiology matters - Genomic DNA methylation patterns in three rat models of acquired epilepsy. *Sci Rep*. 2016;6:25668.
- Casillas-Espinosa PM, Powell KL, Zhu M, et al. Evaluating whole genome sequence data from the Genetic Absence Epilepsy Rat from Strasbourg and its related non-epileptic strain. *PLoS One*. 2017;12(7):e0179924.
- Genome-wide mega-analysis identifies 16 loci and highlights diverse biological mechanisms in the common epilepsies. *Nat Commun*. 2018;9(1):5269.

24. Ellis CA, Petrovski S, Berkovic SF. Epilepsy genetics: clinical impacts and biological insights. *The Lancet Neurology*. 2020; 19(1):93–100.
25. Seyfried NT, Dammer EB, Swarup V, et al. A multi-network approach identifies protein-specific co-expression in asymptomatic and symptomatic Alzheimer's disease. *Cell Syst*. 2017;4(1):60–72.e4.
26. Bitsika V, Duveau V, Simon-Areces J, et al. High-throughput LC-MS/MS proteomic analysis of a mouse model of mesiotemporal lobe epilepsy predicts microglial activation underlying disease development. *J Proteome Res*. 2016;15(5):1546–1562.
27. Schouten M, Bielefeld P, Fratantoni SA, et al. Multi-omics profile of the mouse dentate gyrus after kainic acid-induced status epilepticus. *Sci. Data*. 2016;3:160068.
28. Yang JW, Czech T, Felizardo M, Baumgartner C, Lubec G. Aberrant expression of cytoskeleton proteins in hippocampus from patients with mesial temporal lobe epilepsy. *Amino Acids*. 2006;30(4):477–493.
29. Keren-Aviram G, Dachet F, Bagla S, Balan K, Loeb JA, Dratz EA. Proteomic analysis of human epileptic neocortex predicts vascular and glial changes in epileptic regions. *PloS One*. 2018; 13(4):e0195639.
30. Drummond ES, Nayak S, Ueberheide B, Wisniewski T. Proteomic analysis of neurons microdissected from formalin-fixed, paraffin-embedded Alzheimer's disease brain tissue. *Sci Rep*. 2015;5:15456.
31. Drummond E, Nayak S, Faustin A, et al. Proteomic differences in amyloid plaques in rapidly progressive and sporadic Alzheimer's disease. *Acta Neuropathologica*. 2017;133(6):933–954.
32. David Ellison SL, Chimelli L, Harding BN et al. *Neuropathology: a reference text of CNS pathology*, 3rd ed. MOSBY an imprint of Elsevier Limited: Maryland Heights, MO; 2013.
33. Drummond E, Nayak S, Pires G, Ueberheide B, Wisniewski T. Isolation of Amyloid Plaques and Neurofibrillary Tangles from Archived Alzheimer's Disease Tissue Using Laser-Capture Microdissection for Downstream Proteomics. *Methods Mol Biol (Clifton, NJ)*. 2018;1723:319–334.
34. Cox J, Mann M. MaxQuant enables high peptide identification rates, individualized p.p.b.-range mass accuracies and proteome-wide protein quantification. *Nat Biotechnol*. 2008;26(12):1367–1372.
35. Cox J, Matic I, Hilger M, et al. A practical guide to the MaxQuant computational platform for SILAC-based quantitative proteomics. *Nat Protoc*. 2009;4(5):698–705.
36. Cox J, Michalski A, Mann M. Software lock mass by two-dimensional minimization of peptide mass errors. *J Am Soc Mass Spectrom*. 2011;22(8):1373–1380.
37. Cox J, Hein MY, Luber CA, Paron I, Nagaraj N, Mann M. Accurate proteome-wide label-free quantification by delayed normalization and maximal peptide ratio extraction, termed MaxLFQ. *Mol Cell Proteomics*. 2014;13(9):2513–2526.
38. Tyanova S, Temu T, Sinitcyn P, et al. The Perseus computational platform for comprehensive analysis of (prote)omics data. *Nat Methods*. 2016;13(9):731–740.
39. Szklarczyk D, Franceschini A, Wyder S, et al. STRING v10: protein-protein interaction networks, integrated over the tree of life. *Nucleic Acids Res*. 2015;43(Database)D447–D452.
40. Szklarczyk D, Morris JH, Cook H, et al. The STRING database in 2017: quality-controlled protein-protein association networks, made broadly accessible. *Nucleic Acids Res*. 2017;45(D1):D362–D368.
41. Gu Z, Eils R, Schlesner M. Complex heatmaps reveal patterns and correlations in multidimensional genomic data. *Bioinformatics*. 2016;32(18):2847–2849.
42. Lake BB, Chen S, Sos BC, et al. Integrative single-cell analysis of transcriptional and epigenetic states in the human adult brain. *Nat Biotechnol*. 2018;36(1):70–80.
43. Lleo A, Nunez-Llaves R, Alcolea D, et al. Changes in synaptic proteins precede neurodegeneration markers in preclinical Alzheimer's disease cerebrospinal fluid. *Mol Cell Proteomics*. 2019;18(3):546–560.
44. Dengler CG, Coulter DA. Normal and epilepsy-associated pathologic function of the dentate gyrus. *Prog Brain Res*. 2016;226:155–178.
45. McGuone D, Leitner D, William C, et al. Neuropathologic changes in sudden unexplained death in childhood. *J Neuropathol Exp Neurol*. 2020;79(3):336–346.
46. Fassio A, Esposito A, Kato M, et al.; C4RCD Research Group. De novo mutations of the ATP6V1A gene cause developmental encephalopathy with epilepsy. *Brain*. 2018;141(6):1703–1718.
47. Persike DS, Marques-Carneiro JE, Stein MLL, et al. Altered proteins in the hippocampus of patients with mesial temporal lobe epilepsy. *Pharmaceuticals (Basel)*. 2018;11(4):95.
48. Qin L, Liu X, Liu S, et al. Differentially expressed proteins underlying childhood cortical dysplasia with epilepsy identified by iTRAQ proteomic profiling. *PLoS One*. 2017;12(2):e0172214.
49. Hansen KF, Sakamoto K, Pelz C, Impey S, Obrietan K. Profiling status epilepticus-induced changes in hippocampal RNA expression using high-throughput RNA sequencing. *Sci Rep*. 2014;4:6930.
50. Guelfi S, Botia JA, Thom M, et al. Transcriptomic and genetic analyses reveal potential causal drivers for intractable partial epilepsy. *Brain*. 2019;142(6):1616–1630.
51. Petrovski S, Kury S, Myers CT, et al.; University of Washington Center for Mendelian Genomics. Germline de novo mutations in GNB1 cause severe neurodevelopmental disability, hypotonia, and seizures. *Am J Hum Genet*. 2016;98(5):1001–1010.
52. Hemati P, Revah-Politi A, Bassan H, et al. DDD study. Refining the phenotype associated with GNB1 mutations: clinical data on 18 newly identified patients and review of the literature. *Am J Med Genet A*. 2018;176(11):2259–2275.
53. Tarpey PS, Smith R, Pleasance E, et al. A systematic, large-scale resequencing screen of X-chromosome coding exons in mental retardation. *Nat Genet*. 2009;41(5):535–543.
54. Zhang FX, Sun QJ, Zheng XY, et al. Abnormal expression of synaptophysin, SNAP-25, and synaptotagmin 1 in the hippocampus of kainic acid-exposed rats with behavioral deficits. *Cell Mol Neurobiol*. 2014;34(6):813–824.
55. Zhang MY, Zheng CY, Zou MM, et al. Lamotrigine attenuates deficits in synaptic plasticity and accumulation of amyloid plaques in APP/PS1 transgenic mice. *Neurobiol Aging*. 2014;35(12):2713–2725.
56. Kang JQ. Defects at the crossroads of GABAergic signaling in generalized genetic epilepsies. *Epilepsy Res*. 2017;137:9–18.
57. von Spiczak S, Helbig KL, Shinde DN, et al. EuroEPINOMICS-RES NLES Working Group. encephalopathy: a new disease of vesicle fission. *Neurology*. 2017;89(4):385–394.
58. Walker A, Russmann V, Deeg CA, et al. Proteomic profiling of epileptogenesis in a rat model: focus on inflammation. *Brain Behav Immun*. 2016;53:138–158.
59. Keck M, van Dijk RM, Deeg CA, et al. Proteomic profiling of epileptogenesis in a rat model: focus on cell stress, extracellular matrix and angiogenesis. *Neurobiol Dis*. 2018;112:119–135.
60. You Y, Bai H, Wang C, et al. Myelin damage of hippocampus and cerebral cortex in rat pentylenetetrazol model. *Brain Res*. 2011;1381:208–216.
61. Ye Y, Xiong J, Hu J, et al. Altered hippocampal myelinated fiber integrity in a lithium-pilocarpine model of temporal lobe epilepsy: a histopathological and stereological investigation. *Brain Res*. 2013;1522:76–87.
62. Häberle J, Shahbeck N, Ibrahim K, Hoffmann GF, Ben-Omran T. Natural course of glutamine synthetase deficiency in a 3 year old patient. *Mol Genet Metab*. 2011;103(1):89–91.
63. Eid T, Thomas MJ, Spencer DD, et al. Loss of glutamine synthetase in the human epileptogenic hippocampus: possible mechanism for raised extracellular glutamate in mesial temporal lobe epilepsy. *Lancet*. 2004;363(9402):28–37.

64. Zhou Y, Dhafer R, Parent M, et al. Selective deletion of glutamine synthetase in the mouse cerebral cortex induces glial dysfunction and vascular impairment that precede epilepsy and neurodegeneration. *Neurochem Int.* 2019;123:22–33.
65. Zhou J, Tawk M, Tiziano FD, et al. Spinal muscular atrophy associated with progressive myoclonic epilepsy is caused by mutations in *ASAH1*. *Am J Hum Genet.* Jul. 2012;91(1):5–14.
66. Aronica EM, Gorter JA, Paupard MC, Grooms SY, Bennett MV, Zukin RS. Status epilepticus-induced alterations in metabotropic glutamate receptor expression in young and adult rats. *J Neurosci.* 1997;17(21):8588–8595.
67. Pacheco Otolara LF, Couoh J, Shigamoto R, Zarei MM, Garrido Sanabria ER. Abnormal mGluR2/3 expression in the perforant path termination zones and mossy fibers of chronically epileptic rats. *Brain Res.* 2006;1098(1):170–185.
68. Corti C, Battaglia G, Molinaro G, et al. The use of knock-out mice unravels distinct roles for mGlu2 and mGlu3 metabotropic glutamate receptors in mechanisms of neurodegeneration/neuroprotection. *J Neurosci.* 2007;27(31):8297–8308.
69. Griffin NG, Wang Y, Hulette CM, et al. Differential gene expression in dentate granule cells in mesial temporal lobe epilepsy with and without hippocampal sclerosis. *Epilepsia.* 2016;57(3):376–385.
70. Lionel AC, Vaags AK, Sato D, et al. Rare exonic deletions implicate the synaptic organizer Gephyrin (*GPHN*) in risk for autism, schizophrenia and seizures. *Hum Mol Genet.* 2013;22(10):2055–2066.
71. Dejanovic B, Lal D, Catarino CB, et al. Exonic microdeletions of the gephyrin gene impair GABAergic synaptic inhibition in patients with idiopathic generalized epilepsy. *Neurobiol Dis.* 2014;67:88–96.
72. Förstera B, Belaidi AA, Jüttner R, et al. Irregular RNA splicing curtails postsynaptic gephyrin in the cornu ammonis of patients with epilepsy. *Brain.* 2010;133(Pt 12):3778–3794.
73. Thind KK, Yamawaki R, Phanwar I, Zhang G, Wen X, Buckmaster PS. Initial loss but later excess of GABAergic synapses with dentate granule cells in a rat model of temporal lobe epilepsy. *J Comp Neurol.* 2010;518(5):647–667.
74. de Moura JC, Tirapelli DP, Neder L, et al. Amygdala gene expression of NMDA and GABA(A) receptors in patients with mesial temporal lobe epilepsy. *Hippocampus.* 2012;22(1):92–97.
75. Vlaskamp DRM, Callenbach PMC, Rump P, et al. Copy number variation in a hospital-based cohort of children with epilepsy. *Epilepsia Open.* 2017;22(2):44–254.
76. Meng XF, Yu JT, Song JH, Chi S, Tan L. Role of the mTOR signaling pathway in epilepsy. *J Neurol Sci.* 2013;332(1–2):4–15.
77. Ribierre T, Baulac S. mTOR pathway in familial focal epilepsies. *Oncotarget.* 2017;8(4):5674–5675.
78. Revah-Politi A, Sands TT, Colombo S, et al. *GNB1* encephalopathy. In: Adam MP, Ardinger HH, Pagon RA, et al. eds. *GeneReviews* [Internet]. Seattle (WA); 2020.
79. Barker-Haliski M, White HS. Glutamatergic mechanisms associated with seizures and epilepsy. *Cold Spring Harbor Perspect Med.* 2015;5(8):a022863.
80. Zou J, Wang YX, Dou FF, et al. Glutamine synthetase down-regulation reduces astrocyte protection against glutamate excitotoxicity to neurons. *Neurochem Int.* 2010;56(4):577–584.
81. Thom M. Review: hippocampal sclerosis in epilepsy: a neuropathology review. *Neuropathol Appl Neurobiol.* 2014;40(5):520–543.
82. Punia V, Bena J, Gonzalez-Martinez J, et al. Histopathologic substrate of drug-resistant epilepsy in older adults and the elderly undergoing surgery. *Epilepsia Open.* 2019;4(2):328–333.
83. Nikonenko AG, Radenovic L, Andjus PR, Skibo GG. Structural features of ischemic damage in the hippocampus. *Anat Rec (Hoboken, NJ: 2007).* 2009;292(12):1914–1921.
84. Hatanpaa KJ, Raisanen JM, Herndon E, et al. Hippocampal sclerosis in dementia, epilepsy, and ischemic injury: differential vulnerability of hippocampal subfields. *J Neuropathol Exp Neurol.* 2014;73(2):136–142.
85. Halliday G. Pathology and hippocampal atrophy in Alzheimer's disease. *Lancet Neurol.* 2017;16(11):862–864.
86. Rocca MA, Barkhof F, De Luca J, et al.; MAGNIMS Study Group. The hippocampus in multiple sclerosis. *Lancet Neurol.* 2018;17(10):918–926.
87. Hansen N. Long-term memory dysfunction in limbic encephalitis. *Front Neurol.* 2019;10:330.
88. Gourmaud S, Shou H, Irwin DJ, et al. Alzheimer-like amyloid and tau alterations associated with cognitive deficit in temporal lobe epilepsy. *Brain.* 2020;143(1):191–209.
89. Bartsch T, Wulff P. The hippocampus in aging and disease: from plasticity to vulnerability. *Neuroscience.* 2015;309:1–16.
90. Cole AJ. Is epilepsy a progressive disease? The neurobiological consequences of epilepsy. *Epilepsia.* 2000;41(Suppl 2):S13–S22.
91. Looney MR, Dohan FC, Davies KG, Seidenberg M, Hermann BP, Schweitzer JB. Synaptophysin immunoreactivity in temporal lobe epilepsy-associated hippocampal sclerosis. *Acta Neuropathol.* 1999;98(2):179–185.
92. Kang HC, Lee YM, Kim HD. Mitochondrial disease and epilepsy. *Brain Dev.* 2013;35(8):757–761.
93. DiMauro S, Hirano M, Kaufmann P, et al. Clinical features and genetics of myoclonic epilepsy with ragged red fibers. *Adv Neurol.* 2002;89:217–229.
94. Tryoen-Toth P, Richert S, Sohm B, et al. Proteomic consequences of a human mitochondrial tRNA mutation beyond the frame of mitochondrial translation. *J Biol Chem.* 2003;278(27):24314–24323.
95. Rahman S. Mitochondrial disease and epilepsy. *Dev Med Child Neurol.* 2012;54(5):397–406.
96. Kudin AP, Zsurka G, Elger CE, Kunz WS. Mitochondrial involvement in temporal lobe epilepsy. *Exp Neurol.* 2009;218(2):326–332.
97. Rowley S, Patel M. Mitochondrial involvement and oxidative stress in temporal lobe epilepsy. *Free Radic Biol Med.* 2013;62:121–131.
98. Volmering E, Niehusmann P, Peeva V, et al. Neuropathological signs of inflammation correlate with mitochondrial DNA deletions in mesial temporal lobe epilepsy. *Acta Neuropathol.* 2016;132(2):277–288.
99. Spaulding EL, Burgess RW. Accumulating evidence for axonal translation in neuronal homeostasis. *Front Neurosci.* 2017;11:312.
100. Hodges SL, Lugo JN. Therapeutic role of targeting mTOR signaling and neuroinflammation in epilepsy. *Epilepsy Res.* 2020;161:106282.
101. Kim JK, Cho J, Kim SH, et al. Brain somatic mutations in *MTOR* reveal translational dysregulations underlying intractable focal epilepsy. *J Clin Invest.* 2019;129(10):4207–4223.
102. Pernice HF, Schieweck R, Kiebler MA, Popper B. mTOR and MAPK: from localized translation control to epilepsy. *BMC Neurosci.* 2016;17(1):73.
103. Marinissen MJ, Gutkind JS. G-protein-coupled receptors and signaling networks: emerging paradigms. *Trends Pharmacol Sci.* 2001;22(7):368–376.
104. Yu Y, Nguyen DT, Jiang J. G protein-coupled receptors in acquired epilepsy: druggability and translatability. *Prog Neurobiol.* 2019;183:101682.
105. Steinrucke S, Lohmann K, Domingo A, et al. Novel *GNB1* missense mutation in a patient with generalized dystonia, hypotonia, and intellectual disability. *Neurol Genet.* 2016;2(5):e106.
106. Lohmann K, Masuho I, Patil DN, et al. Novel *GNB1* mutations disrupt assembly and function of G protein heterotrimers and

- cause global developmental delay in humans. *Hum Mol Genet.* 2017;26(6):1078–1086.
107. Jones HF, Morales-Briceno H, Barwick K, et al. Myoclonus-dystonia caused by GNB1 mutation responsive to deep brain stimulation. *Mov Dis.* 2019;34(7):1079–1080.
  108. Endo W, Ikemoto S, Togashi N, et al. Phenotype-genotype correlations in patients with GNB1 gene variants, including the first three reported Japanese patients to exhibit spastic diplegia, dyskinetic quadriplegia, and infantile spasms. *Brain Dev.* 2020;42(2):199–204.
  109. Colombo S, Petri S, Shalomov B, et al. G Protein-Coupled Potassium Channels Implicated in Mouse and Cellular Models of GNB1 Encephalopathy. 2019;697235, doi:10.1101/697235 %JbioRxiv
  110. Sriram K, Insel PA. G protein-coupled receptors as targets for approved drugs: how many targets and how many drugs? *Mol Pharmacol.* 2018;93(4):251–258.
  111. Czapiński P, Blaszczyk B, Czuczwar SJ. Mechanisms of action of antiepileptic drugs. *Curr Topics Med Chem.* 2005;5(1):3–14.